Climate Change, Predator-Prey Interactions, and Population Dynamics of the Ranchman's Tiger Moth (*Arctia virginalis*)

By

ADAM ALESSANDRO PEPI

DISSERTATION

Submitted in partial satisfaction of requirements for the degree of

DOCTOR OF PHILOSOPHY

in

Ecology

in the

OFFICE OF GRADUATE STUDIES

of the

UNIVERSITY OF CALIFORNIA

DAVIS

Approved:

Richard Karban, Co-Chair

Marcel Holyoak, Co-Chair

Jay Rosenheim

Eric Post

Committee in Charge

2021

Dedication

To my wife, Julia

Table of Contents

Acknowledgements

First, I would like to thank my advisors, Richard Karban and Marcel Holyoak, who have supported me admirably throughout graduate school: materially, professionally, and as friends.

I also would like to thank my dissertation and qualifying committee members: Jay Rosenheim, Louie Yang, Susan Harrison, James Griesemer, and Eric Post. All of you have greatly enriched my experience at Davis, and provided essential support to my research and scholarship.

I would like to thank labmates Patrick Grof-Tisza, Eric LoPresti, Danielle Rutkowski, Naomi Murray, and Vincent Pan for being great companions and support during all of my time at Davis. My work would have been impossible and my experience much impoverished without you.

I would like to thank also the many undergraduates who worked with me on my projects: Fiona Beyerle, Isabel Gilchrist, Gina Mongiello-Lopez, Jasmine Daragahi and Claire Beck, Vinay Mase, Aiyanna Laws-McNeil, Cameron Moseley and Alexis Ballman. Many other staff at Davis or other places where I conducted my field work also greatly supported my work, but I want to thank Jackie Sones first among them for supporting my work over all these years at Bodega Marine Reserve.

Lastly I would like to thank friends and collaborators for making my time at Davis incalculably better: Marshall McMunn, Amy Miles, Yuzo Yanagitsuru, Will Hemstrom, Helen Killeen, Matt Thorstensen, Tracie Hayes, and Kelsey Lyberger.

Abstract

In my dissertation, I examined how a changing environment affects Ranchman's tiger moth (*Arctia virginalis*) population dynamics via predator-prey and host-pathogen interactions. I also examined the complex ways in which biotic drivers of population dynamics interact with climate forcing.

In **Chapter 1**, I examined how body size mediates the effect of warming on the interaction between *Arctia virginalis* and an ant predator (*Formica lasioides*). I also developed a general framework for understanding warming effects on stage or size-dependent predator-prey interactions. Specifically, I showed through experiments and modelling that *A. virginalis* is only vulnerable to predation by *F. lasioides* when small. This window of vulnerability narrows as the development rate of *A. virginalis* increases with warming. However, the attack rate of *F. lasioides* also increases with warming and overcompensates for the decreasing window of prey vulnerability. We therefore project warming to favor the predator in this case, in contrast to the results of previous related work in other systems.

In **Chapter 2**, I expanded upon Chapter 1 by examining the effects of warming on predator-prey interactions in multi-predator communities. In Chapter 1, I showed that asymmetries in predator-prey thermal response rates can result in changing interactions, constituting an important indirect effect of warming. In demographic models using simulated and empirically informed parameters from a natural community of ant predators, I showed that greater predator diversity paired with sufficient thermal niche diversity attenuates these indirect effects of warming, leaving only direct, physiological effects. This result depends on predator diversity and thermal niche diversity and complementarity, which has significant implications for

how we might expect warming to affect predator-prey interactions in different communities dependent on traits of the community thermal niche.

In **Chapter 3**, I examined viral disease as a mechanism for delayed density-dependent dynamics in *A. virginalis* populations and the role of ultraviolet radiation in reducing viral infection through attenuating virions persisting in the environment. I censused 18 populations across 9° of latitude and a gradient of ultraviolet radiation intensity for two years and measured viral infection rate, severity, and survival of lab-reared caterpillars. I found that caterpillar density in the previous year led to a higher infection rate and severity and lower survival and that ultraviolet radiation led to lower infection severity and higher survival. This suggested that virus is the main mechanism for cyclic dynamics in this species, which has been proposed theoretically but rarely shown empirically. I also found a population-level effect of ultraviolet radiation on viral infection severity, which had not been shown previously.

In **Chapter 4**, I analyzed long-term *A. virginalis* census data, finding that changing precipitation patterns due to changes in large-scale climate led to qualitative changes in population dynamics. Using change-point analysis and state-space models, I showed that caterpillar dynamics transitioned from short to long-period dynamics concurrent with a change in precipitation dynamics. Using deterministic simulations, I showed that shifting dynamics were likely due to resonance: precipitation patterns interfered with cycles initially and later amplified cycles.

1. Introduction

Climate change has profound effects on ecological communities (Walther et al. 2002, Parmesan 2006), and the impact of climate change on population dynamics is a key element of those effects. Climate effects on population dynamics can be direct via organismal physiology, or indirect via biotic interactions (Tylianakis et al. 2008). One of the main drivers of direct effects of climate change is warming (Uszko et al. 2017), which affects metabolic rate in ectotherms. Increasing metabolic rates can have predictable direct effects on organisms, though they are complex and depend greatly on details of life history. A large proportion of the impacts of changing climate on population and community dynamics is likely due to indirect effects, via changing interspecific interactions (Tylianakis et al. 2008, Post 2013). This can be due to changes in phenology causing match or mismatch between species (Post and Forchhammer 2002), range shifts resulting in new combinations of interacting species (Parmesan 2006), or effects of climate change on the interactions themselves.

Climate effects have been observed or predicted on a wide range of biotic interactions, including facilitative interactions such as plant-plant mutualisms (Brooker 2006) and pollination (Scaven and Rafferty 2013), as well as competitive interactions (Brooker 2006, Lang et al. 2012), herbivory (Zvereva and Kozlov 2006), predator-prey (Ohlund et al. 2014, Culler et al. 2015, Uszko et al. 2017), parasitoid-host (Jeffs and Lewis 2013, Duan et al. 2014), and host-pathogen interactions (Elderd and Reilly 2014). The amount of research examining climate effects on these different types of interactions varies widely, with pollination for example having no known studies of climate effects on interactions other than due to phenology or range shifts (Scaven and Rafferty 2013) and very few examples for parasitism (Jeffs and Lewis 2013, Duan et al. 2014). Climate effects on predator-prey interactions by contrast have been the subject of a

number of experimental (e.g., Barton and Schmitz 2009, Culler et al. 2015) and modelling studies (e.g., Rall et al. 2010, Dell et al. 2014, Uszko et al. 2017). This developing body of work offers the potential to help predict how climate change will affect predator-prey interactions, which are key factors affecting community dynamics and ecosystem functioning (Chapin et al. 1997).

Besides understanding how climate change will affect population dynamics through direct vs. indirect pathways, understanding how climate will interact with complex population dynamics is a key component of understanding climate impacts on the biosphere. Population cycles are a prominent phenomenon which has been a focus of ecological research since the inception of the field (Elton and Nicholson 1942, Turchin 2003, Barraquand et al. 2017). Population cycles are often thought to be driven by trophic interactions (Berryman 2002, Turchin 2003), which have the potential to be impacted by climate change. Some work has suggested that climate warming may be leading to collapsing population cycles (Killengreen and Ims 2008, Cornulier et al. 2013), while in other cases warming has led to disrupted population regulation and the renewal of cyclic pest outbreaks (Ward et al. 2020). Climate change has also resulted not just in changes in mean climate, but also in changes to patterns of climate variation (Coumou and Rahmstorf 2012, Simon Wang et al. 2017). These changes in the pattern of climate variation can interact with the density-dependent feedback structure of population dynamics and lead to complex changes to dynamics (Royama 1992, Greenman and Benton 2003, Barraquand et al. 2017).

Over the past several decades, ecologists have characterized a wide range of mechanisms through which climate change may impact the biosphere, only some of which I have reviewed. As I see it, an important next step for the field is to bring together these observations and try to

develop theory to predict how we expect these impacts to manifest across natural systems. There have been advances in metabolic theory and range limit theory that both can be utilized to generate predictions about how we expect impacts of climate change to vary geographically (e.g., Deutsch et al. 2008, Louthan et al. 2015). My dissertation consists of a mixture of characterization of biotic components of population dynamics (predation, disease), environmental impacts on biotic interactions (warming, precipitation, ultraviolet radiation), and developing theory to predict how the relative importance of direct vs. indirect effects of warming may vary between communities. However, I see this as only the beginning, and in the process of conducting my dissertation research I have found myself interested in pursuing multiple further avenues of work which I believe have great potential to increase our understanding of the biotic impacts of climate change.

In Chapter I, I examine size and temperature-dependent predator-prey interactions between *Arctia virginalis* and its ant predator, *Formica lasioides*, and develop a mathematical modelling framework to understand the effects of warming on this interaction. This work is published in *Ecology*. In Chapter II, I expand this work into multi-species communities, and develop theoretical predictions with regard to which combinations of community thermal traits will lead to stronger direct vs. indirect effects of warming. This work is in published in *The American Naturalist*. In Chapter III, I examine the role of viral disease and its attenuation by ultraviolet radiation in cyclic population dynamics of *Arctia virginalis.* This forms the basis of Chapter IV, in which I examine how changing precipitation patterns in California interact with disease-driven density-dependent feedbacks in *Arctia virginalis* population dynamics, resulting in shifting dynamics, from short-period cycles or no cycles, to clearer, long-period cycles. This work is published in *Ecology Letters*.

2. Chapter I: As temperature increases, predator attack rate is more important to survival than a smaller window of prey vulnerability

As published in *Ecology* with Patrick Grof-Tisza, Marcel Holyoak and Rick Karban (Pepi et al. 2018)

2.1 Abstract

Climate change can have strong effects on species interactions and community structure. Temperature-dependent effects on predator-prey interactions are a major mechanism through which these effects occur. To understand the net effects of predator attack rates and dynamic windows of prey vulnerability, we examined the impacts of temperature on the interaction of a caterpillar (*Arctia virginalis*) and its ant predator (*Formica lasioides*). We conducted field experiments to examine attack rates on caterpillars relative to temperature, ant abundance, and body size, and laboratory experiments to determine the effects of temperature on caterpillar growth. We modeled temperature-dependent survival based on the integrated effects of temperature-dependent growth and temperature- and size-dependent predation. Attack rates on caterpillars increased with warming and ant recruitment, but decreased with size. Caterpillar growth rates increased with temperature, narrowing the window of vulnerability. The model predicted net caterpillar survival would decrease with temperature, suggesting *A. virginalis* populations could be depressed with future climate warming. Theoretical work suggests the net outcome of predator-prey interactions with increasing temperature depends on the respective responses of interacting species in terms of velocity across space, whereas the present study suggests the importance of effects of temperature on prey window of vulnerability, or 'velocity' across time.

2.2 Introduction

Climate change is causing widespread alteration to species' ranges, life histories, and phenologies (Parmesan 2006). These changes impact species interactions, population dynamics, and ultimately, community structure and function (Cramer et al. 2001, Tylianakis et al. 2008). Altered phenologies have received the most study but climate change can also have direct impacts on interactions, independent of phenological effects (Tylianakis et al. 2008). There are various mechanisms through which climate change can affect species interactions, but the effects of temperature are particularly pervasive due to the strong effects of temperature on metabolism. While all aerobic organisms have the same basic biochemical mechanisms of metabolism, ectotherms which have metabolic rates directly tied to ambient temperatures make up a majority of the planet's biodiversity and biomass (Gillooly et al. 2001). Increased metabolic rates can cause increased attack rates by predators (Rall et al. 2010); this can in turn cause increased interaction strength with prey, leading ultimately to changes in density or dynamics of prey and to cascading effects on broader community structure (Berlow et al. 2009, Petchey et al. 2010). Temperature-augmented metabolic rates can also result in increased growth rates of prey (Kingsolver et al. 2011), which can also have broader effects through altered interactions with predators (Benrey and Denno 1997, Culler et al. 2015). For example, larger prey are often less vulnerable to predation and temperature-augmented growth rates decrease the time for prey to reach a size refuge.

A body of theoretical work has investigated the effects of warming on ectothermic predator-prey systems (Dell et al. 2014, Uszko et al. 2017). Modeling and experimental studies make diverse predictions, depending on model assumptions or system-specific temperature responses. These predictions include increased population stability (Fussmann et al. 2014),

decreased stability (Beisner et al. 1997, Vasseur and McCann 2005), extinction (Petchey et al. 2010, Rall et al. 2010, Vucic-Pestic et al. 2011), increased top-down control (O'Connor et al. 2009, Hoekman 2010), or complex responses to temperature in predator-prey systems (Amarasekare 2015). These varied predictions have more recently been synthesized in a unified model based on assumptions about the effects of temperature on carrying capacity and predator performance (Uszko et al. 2017). This body of work is largely founded on laboratory and microcosm studies, which has repeatedly shown that increased temperatures result in increased predation rates by invertebrate predators (e.g., Rall et al. 2010, Vucic-Pestic et al. 2010, Culler et al. 2015, Karban et al. 2015) at least within a 'biologically relevant temperature range'(Englund et al. 2011) before thermal performance maxima are reached. However, fewer studies have tested the effects of increased temperature on predation rates in the field (but see Barton and Schmitz 2009).

Besides predator attack rates, temperature can have strong effects on prey development rates. This can in turn have strong effects on prey survival. The slow-growth-high-mortality hypothesis (Benrey and Denno 1997) proposes that longer development times can expose vulnerable stages of insects to natural enemies for a longer time, resulting in higher mortality. If vulnerability to predation varies with ontogeny, the more rapid escape of prey from vulnerable stages can potentially offset increased predator attack rates entirely. Variable vulnerability to predation over ontogeny can occur through various mechanisms. Juveniles of taxa that undergo metamorphosis may be more vulnerable than adults and thus will experience less predation risk if they reach adulthood faster (Culler et al. 2015). Consumption of prey is often size-dependent, sometimes due to gape-limited predators, such that if prey grow faster they will reach a size refuge at which predation risk is minimal (Anderson et al. 2001, Taylor and Collie 2003).

Because a wide range of taxa may have both stage or size-dependent predation risk and have temperature-dependent growth it is important to examine the combined effects of increased attack rates by predators and increased development rate of prey to understand the net effect of temperature on predator-prey systems.

In this study we examined the effect of experimental warming on the interaction between the ant *Formica lasioides* and its prey, caterpillars of the tiger moth, *Arctia virginalis* (formerly *Platyprepia virginalis*). Previous long-term work on *A. virginalis* at Bodega Marine Reserve, Sonoma, California, has shown large annual fluctuations in caterpillar densities (Karban and de Valpine 2010), and suggested that precipitation and ant predation may be important drivers of observed dynamics (Karban et al. 2017). Ant predation has been shown in the laboratory to be affected by temperature (Karban et al. 2015), and by the depth and quality of litter substrate (Karban et al. 2013). The region where these studies have been conducted, the central coast of California, is expected to become warmer and drier with future climate change (Weare 2009, Li et al. 2014). Given these climate projections and the importance of temperature for this system, we expect that *A. virginalis* dynamics will change as a result of increased predator attack rate and accelerated larval development at warmer temperatures. We tested the effects of experimental warming on this interaction in the field and laboratory, and created a model using our experimental data to help understand how these interacting climate-driven factors are likely to impact the dynamics of *A. virginalis*.

2.3 Methods

Warming tent predation experiment

To determine the effects of temperature on caterpillar predation by ants in the field, we exposed caterpillars in enclosures to ants inside and outside warming tents. Experimental

warming tents were constructed at Bodega Marine Reserve, Sonoma, California (38°19'7.16"N, 123° 4'17.43"W) on 17-18 July 2017. Ten tents, measuring 2x2x2 m were constructed at or near long-term monitoring plots for *A. virginalis* caterpillars. Tents were domes with PVC frames covered by clear polyethylene plastic sheeting (6 mil, Home Depot, Atlanta, Georgia) on their sides up to 1 m and open tops. On 18 July, four deli containers (11 cm diameter), each with 3 second instar *A. virginalis* caterpillars and approximately 1 g of fresh lupine (*Lupinus arboreus*) flowers were placed inside and an equal number were placed 0.5 m outside the tents. Containers had window screen bottoms that allowed ants to enter and leave but prevented caterpillars from leaving. Temperature loggers (iButton, Maxim Integrated, San Jose, CA) were placed inside and outside of each tent at the same time and recorded temperatures every hour. On 21 July, the number of missing caterpillars in each container was recorded (Trial 1), any missing or dead caterpillars were replaced, and fresh lupine petals were added to each container. To account for spatial variation of ant density, we recorded the number of ants recruiting to bait stations to use as a covariate in our model. This was calculated as the total number of ants recruiting to bait at each tent site, both inside and outside of tents. Ant baits consisting of super saturated sugar-water soaked cotton balls on petri dishes were placed out at the same time at sites, inside and outside of each tent. These baits were revisited after several hours when the number of *F. lasioides* recruiting to bait was recorded. We have previously found that when caterpillars are placed out in the field they were usually discovered and killed by ants within a few hours or remained safe for the duration. On 24 July, the number of missing caterpillars in containers was measured for a second time (Trial 2), and temperature loggers were retrieved. Since caterpillars were too large to leave the containers, any missing caterpillars were assumed to have been killed and consumed

by ant predators. We have observed ants killing, dismembering, and removing these dismembered caterpillars from our experimental containers on many occasions.

Data were analyzed using mixed effects models in R (v. 3.4.3), using the lme4 package (Bates et al. 2014). All models included site (tent location) as a random effect. The average warming effect of tents was assessed using daytime temperature measurements, from 7 a.m. to 9 p.m., in a linear mixed effects model. The effect of warming treatment on ant recruitment was tested with a Poisson mixed model, with trial included as a fixed effect, and an individual level random effect to account for overdispersion (i.e., each replicate was a level in the random effect, see Harrison 2014). Predation on caterpillars by warming treatment was assessed using a binomial mixed model, with total number of *F. lasioides* recruiting to baits at each site, trial, an interaction between treatment and ant recruitment, and an individual level random effect to account for overdispersion included as predictors.

Temperature-dependent growth experiment

To assess the effects of temperature on caterpillar growth rates, we reared early instar caterpillars in the laboratory over a range of temperatures. On 6 June 2017, caterpillars, each weighing 1 or 2 mg, were placed in individual vented plastic containers (7 cm diameter condiment cups) and reared in growth chambers at constant temperatures of 10°, 15°, 20°, and 25° C. These temperatures reflect the natural range of summer temperatures at Bodega Bay (July & August avg. daily min 11° C- max 15° C) and temperatures in the field warming experiment (avg. 21.7° C control & 22.9° C warming). Fifty-two caterpillars were reared at each temperature. Caterpillars were fed organic romaine lettuce and occasional lupine petals and foliage every three days. Caterpillars were weighed every three weeks, with a total of 4 subsequent weighings ending on 26 August 2017. Individual growth rates from each weighing

period to the next were calculated for each caterpillar as $\ln(W_t/W_{t+1})$. The dependence of caterpillar growth rate on temperature as a categorical predictor was tested using a mixed effects model, with weighing date as a random effect. Temperature as a continuous predictor was also included in a second linear model of caterpillar growth rate.

Size dependent predation experiment

To measure the effects of caterpillar size on predation rates in the field, we conducted experiments exposing caterpillars of different sizes to ant predators. Lab-reared caterpillars ranging from 10 to 571 mg of weight were placed singly in mesh-screened deli containers (11-cm diameter) at Bodega Bay Marine Reserve to assess size-dependent predation rates. Caterpillars could not escape through the mesh although ants were able to enter and leave. Sixty-six caterpillars were deployed on 13 August 2017 and retrieved after 6 days, and 81 caterpillars were deployed on 27 August and retrieved after 7 days. Caterpillars were counted as consumed or survived when deli containers were recovered. Survival was compared to the log of caterpillar weight with and without trial as a covariate in a binomial generalized linear model.

Model of temperature-dependent survival

A model of temperature-dependent survival of caterpillars was constructed to assess survival as affected by temperature-dependent growth, predation, and size-dependent predation. Functions of daily growth and predation rates by temperature, and size-dependent predation were derived from data using generalized linear models. Size-dependent predation was expressed as a fraction of the maximum predation rate by size, which was for the smallest individuals. Data for temperature-dependent predation were from Karban et al. (2015), but modeled with temperature as a continuous predictor in a binomial generalized linear model. The form of the model of temperature-dependent survival was as follows:

$$P = \prod_{i=1}^{n} \frac{\exp\left\{a\left(x_0^{r(T)t_i}\right)\right\}}{1+\exp\left\{a\left(x_0^{r(T)t_i}\right)\right\}} \left(\frac{\exp\{b(T)\}}{1+\exp\{b(T)\}}\right) \quad (1)$$

where t is time in days, x_0 is initial caterpillar weight (10 mg), T is temperature, r is instantaneous daily caterpillar growth rate as a function of temperature, a represents size-dependent daily predation, and b is daily temperature-dependent predation rate. The first term is the inverse logit transformed size-dependent predation rate derived from a binomial model, with caterpillar size growing each day at a temperature dependent rate. The second term is the inverse logit transformed temperature-dependent predation rate also derived from a binomial model (see S1). The model calculates the daily temperature and size-dependent predation risk of a caterpillar that is iteratively grown at a temperature dependent growth rate. The predation risk of each day is then multiplied together to determine predation risk across the entire larval stage. The product of the daily predation risk of each consecutive day was generated for values of caterpillar weights less than 400 mg ($x_0^{r(T)t}<400$) for temperatures from 10 to 25° C.

To illustrate the relative contribution of the different components of the model to larval predation risk with temperature, sensitivity analyses were conducted. Versions of the model without size-dependent predation, temperature-dependent growth, and temperature-dependent predation were run. For the model without size-dependent predation risk, the full predation rates from the smallest caterpillars as used in the laboratory temperature-dependent predation trials were used for all caterpillar sizes. For the model without temperature-dependent growth, the growth rate of caterpillars was fixed at that measured for 10° C. For the model without temperature-dependent predation, the predation rate was fixed at the rate measured in the laboratory at 10° C, though still modified by increasing caterpillar size.

2.4 Results

The tents were successful at raising daytime temperatures at ground level. The ground temperature inside of tents was 1.2° C (±0.4°C) above average ambient temperature (β=0.77 [95% CI:0.6-0.88], t=3.0, p=0.002). These elevated temperatures are conservative relative to climate change models of coastal California for the near future, with one study projecting 2° C of warming by the 2060s (Li et al. 2014).

Rates of predation were affected by elevated temperatures in the field experiment. After controlling for ant density, caterpillars were more likely to survive at ambient temperatures than at elevated temperatures in both experimental trials (Figure 2.1). Predation of caterpillars by ants was significantly higher in trial 2 in both treatments than in trial 1 (β=0.2 [95% CI:0.09-0.35], z=-3.4, p<0.001, Figure 2.1). There was a significant interaction between total *F. lasioides* recruiting to baits and treatment effect in both trials (β=0.49 [95% CI: 0.48-0.50], z=-2.76, p=0.02, Figure 2.1). This means that at higher rates of ant recruitment, survival of caterpillars in the warming treatment became lower than controls. Ant recruitment to baits was not affected by elevated temperatures in the field experiment (p>0.05).

Caterpillar survival rates in size-dependent field predation trials increased significantly with log caterpillar weight (β=0.76 [95% CI: 0.38-0.46], df=106, z=3.17, p=0.001, Figure 2.2a), and were not significantly different between trials. Caterpillar growth rates were significantly higher at higher temperatures (mixed model: χ^2= 214.5, p<0.001; linear model: β=0.058±0.005, df=547, t=11.33, p<0.001, Figure 2.2b) and caterpillar survival rates in laboratory predation trials were significantly lower at higher temperatures (β=0.76 [95% CI: 0.54-0.91], df=146, z=-4.15, p<0.001, Figure 2.2c).

In the model of temperature-dependent generation survival, caterpillar survival continuously declined with increasing temperature (Figure 2.2d). This model included temperature-dependent caterpillar growth as well as temperature- and size-dependent predation rates. The sensitivity analyses illustrated that size- and temperature-dependent predation rates had the largest impact on caterpillar survival (Figure 2.3). In the model without size-dependent predation, caterpillar survival was much lower and declined quickly to zero. In the model without temperature-dependent predation, caterpillar survival was higher and increased with temperature. In the model without temperature dependent growth, caterpillar survival declined somewhat more quickly with temperature than the full model.

2.5 Discussion

The warming experiment showed that caterpillar predation by ants was higher with experimentally elevated temperature under field conditions. The interaction between ant recruitment and caterpillar survival demonstrated that the effect of the warming treatment on caterpillar survival was due to ant predation; caterpillar survival was lower in warming tents than controls only when ants were present, and this effect was stronger with increasing ant abundance. The decreasing rate of predation with caterpillar body size provides a mechanism by which temperature via increased body growth rates can increase overall survival. However, the integrated model of caterpillar survival (equation 1) showed that the net effect of warmer temperatures was negative for caterpillars; increased growth and lower predation at larger caterpillar size did not compensate for increased attack rates with higher temperature, leading to decreasing survival with temperature. This contrasts with other studies in which prey growth rates increased enough with temperature that prey species reached a size refuge fast enough to overcompensate for the increased attack rates of ectothermic predators, leading to increasing

prey survival with temperature (Anderson et al. 2001, Taylor and Collie 2003). The relative effects of temperature on predator attack rate and prey window of vulnerability determined the net effect of temperature on the predator-prey interaction. This is seen in the sensitivity analyses (Fig. 2.3), where the removal of the temperature-dependence of the predator attack rate had a much larger effect on caterpillar survival than removing temperature-dependence of the growth rate. This result suggests that the comparison of positive effects on prey growth but negative effects of predation is important to understand the effects of temperature on predator-prey interactions.

In this study we measured an overall predation rate rather than a per-individual attack rate as typically measured in laboratory studies (e.g. Vucic-Pestic et al. 2011). This means that we sacrifice precision in our ability to calculate the per capita effects of temperature on predators in favor of ecological realism. However, our statistical model of the field warming experiment includes ant recruitment to baits as an index of ant density, so the significant interaction between the effects of ant recruitment and warming treatment on caterpillar survival shows that for a given index of ant abundance, attack rates are higher with higher temperatures. Furthermore, temperature dependent increases in attack rate may be caused both by higher activity rates and by faster gut evacuation times (Vucic-Pestic et al. 2011). *Formica lasiodes* is a colonial species which brings most foraged food items back to the colony and does not directly consume food acquired, so temperature-dependent gut evacuation time is unlikely to be relevant in this case. Therefore we assume that higher activity rate is the mechanism driving increases in attack rate in this system.

In this work, we assume ad-libitum food access for growing caterpillars in the field; this assumption is typically true of later instar caterpillars (Karban et al, 2017). However, this may

not be the case in the summer when early instars are developing, given highly variable precipitation in California. Organisms with limited food resources are likely to have unimodal responses of growth rate to temperature, where the maximum growth rate is below maximum metabolic rate (Elliott 1982). This violates our assumption of linearly increasing growth rates with temperature, and would likely increase the observed negative impact of temperature on caterpillar survival rates. Increased temperatures also have the potential effect of decreasing adult sizes even while increasing growth rates (Sweeney et al. 2018). Our work does not consider such possible effects; however a larval size refuge is reached at sizes considerably lower than normal pupation weights (Fig. 2.2a), so this process is unlikely to affect predation rate by ants. Decreased adult body sizes caused by increasing temperatures however could potentially negatively affect population growth rates due to lowered adult fecundity as has been suggested in other system (Sweeney et al. 2018); in the present paper however we focus on predator-prey interactions within the larval stage.

The increase in predation rate (ca. 75%) at sites with higher ant densities that resulted from a relatively small amount of warming (avg. 1.2° C) in the field experiment suggests that climate warming could result in increased top-down control of caterpillars. This matches the predictions of some previous work regarding temperature-dependent effects on predator-prey interactions (O'Connor et al. 2009, Hoekman 2010). If the future climate of coastal California is warmer and drier as models have predicted (Weare 2009, Li et al. 2014), populations of *A. virginalis* could be depressed relative to current levels. Models and experiments presented here predict increased predation by ants due to augmented attack rates associated with higher temperature. Previous work that focused on expectations of lower future precipitation predicted

higher predation by ants due to higher ant densities and fewer refuges for caterpillars (Karban et al. 2017).

Similar work comparing the net effects of temperature-augmented predation versus development rates on survival rates in Arctic mosquitoes (Culler et al. 2015) suggested that at higher temperatures mosquitoes would have higher survival, ultimately resulting in higher mosquito populations and impacts on ungulates in the surrounding ecosystem. Work on damselfly larvae feeding on larval amphibians similarly showed that faster tadpole growth allowed prey to escape predators and attain higher survival rates at higher temperatures (Anderson et al. 2001). Another study examining sand shrimp preying on larval winter flounder found similarly that winter flounder escaped stages vulnerable to sand shrimp faster, though these benefits to flounder disappeared at higher temperatures (Taylor and Collie 2003). The present study, in contrast, found an opposing result, that increased growth rates of prey did not compensate for higher attack rates of predators.

Modeling work has suggested that the relative response rates of predators and prey to temperature will determine the outcome of predator-prey interactions (Dell et al. 2014, Ohlund et al. 2014). However, such work has thus far only considered the effects of temperature on the velocity of predator and prey movements and not effects of augmented prey growth rate on the window of prey vulnerability. Many ectothermic species are likely to experience stage or size-dependent predation. Stage-dependent predation has been found to be important for many insects and amphibians that have complex lifecycles and undergo metamorphosis (Werner 1986, Benrey and Denno 1997), whereas size-dependent predation is probably important for many taxa but has been best documented in aquatic systems (e.g., Paine 1976, Mittelbach 1981, Christensen 1996). Since these effects may be common in ectothermic species, the effect of temperature

through increased prey growth rates on the window of vulnerability, or the 'velocity' of prey through time as a means of escaping predators, is a good candidate to be included in future models of predator-prey interactions.

Besides size- and stage-dependent predation, complex lifecycles are an important life-history trait that is likely to impact the effects of temperature on population dynamics, but they have not generally been examined in theoretical work. This is probably because the temperature-dependent responses of growth and survival of ectothermic organisms with complex lifecycles are not well understood (Kingsolver et al. 2011). Species with complex lifecycles often undergo ontogenetic niche shifts (such as *A. virginalis*, Grof-Tisza et al. 2014) and experience different abiotic and biotic environments during different stages. In addition, different life stages can be differentially sensitive to temperature (Amarasekare and Sifuentes 2012). As such, the effects of temperature on species with complex lifecycles relative to those of their predators or prey are likely to be hard to predict in generalized temperature-dependent predator-prey models. Analyses thus far have not examined broader patterns of temperature effects on organisms with complex lifecycles to identify key factors or traits that affect survivorship and growth rate. One study examining three species suggested that the most temperature-sensitive life stage should have the greatest effect on survivorship (Amarasekare and Sifuentes 2012). The effects of some traits on temperature-dependent predator-prey interactions however have been considered in theoretical and experimental work: predator size (Brose 2010, Rall et al. 2010) and predator hunting mode (Barton and Schmitz 2009, Dell et al. 2014) are both important factors that impact how temperature affects predator-prey population dynamics.

In summary, this study represents a rare field demonstration showing increased attack rates by an ectothermic predator on its prey at higher temperature in which the net outcome is

dependent on the relative impact of temperature on predator attack rates and prey window of vulnerability. Our analysis which considered temperature-augmented prey growth differed from other similar studies by finding a negative net outcome for the prey associated with biologically relevant elevated temperature according to future climate predictions. That increased temperature can increase attack rates of predatory ectotherms is a key assumption of a growing body of modeling literature, which has thus far mostly relied on laboratory and microcosm work; these data are not always accurate representations of how species and interactions will perform *in situ*. This and other studies that included the effects of temperature on prey window of vulnerability show that this is an important factor that might influence the net effects of temperature in many predator-prey systems. Finally, more field experiments and detailed work considering the broader effects of temperature on predator-prey interactions will better serve to test the predictions of existing theoretical and laboratory work on the effects of climate warming on predator-prey systems. This will help solidify our understanding of how climate warming is likely to reshape ecological communities through altering these interactions.

2.6 Acknowledgements

We thank Eric LoPresti for help with caterpillar rearing, and Andrew Ross, Louie Yang, and Jay Rosenheim for use of growth chambers. This study was conducted in part at Bodega Marine Reserve and Jackie Sones facilitated our fieldwork there. This work was supported by NSF-LTREB-1456225.

2.7 Tables & Figures

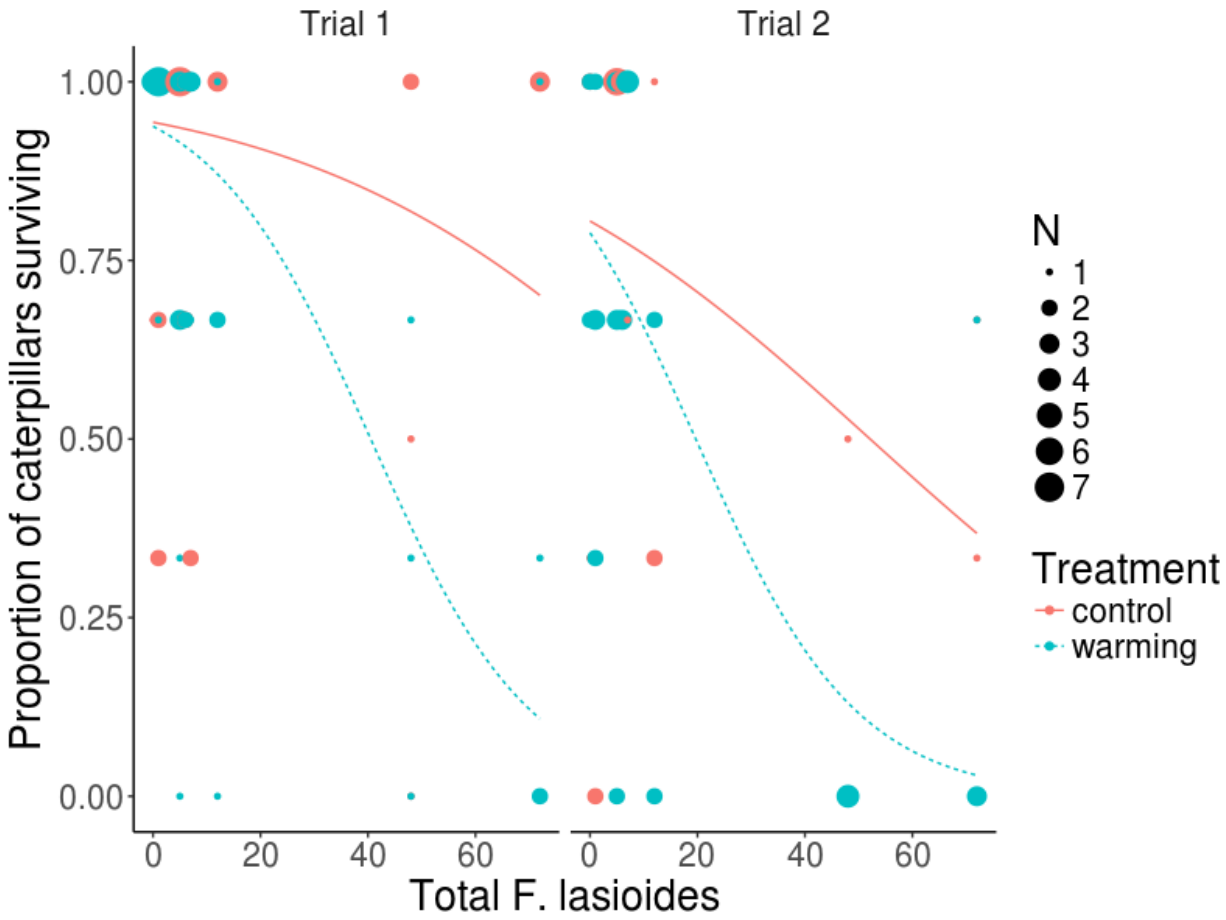

Figure 2.1. Proportion of caterpillars remaining in deli containers by treatment (red: controls, blue: warming), and number of *Formica lasioides* recruiting to baits at each container. Proportions are out of three caterpillars, and the number of samples falling on each position is represented by the size of the circle.

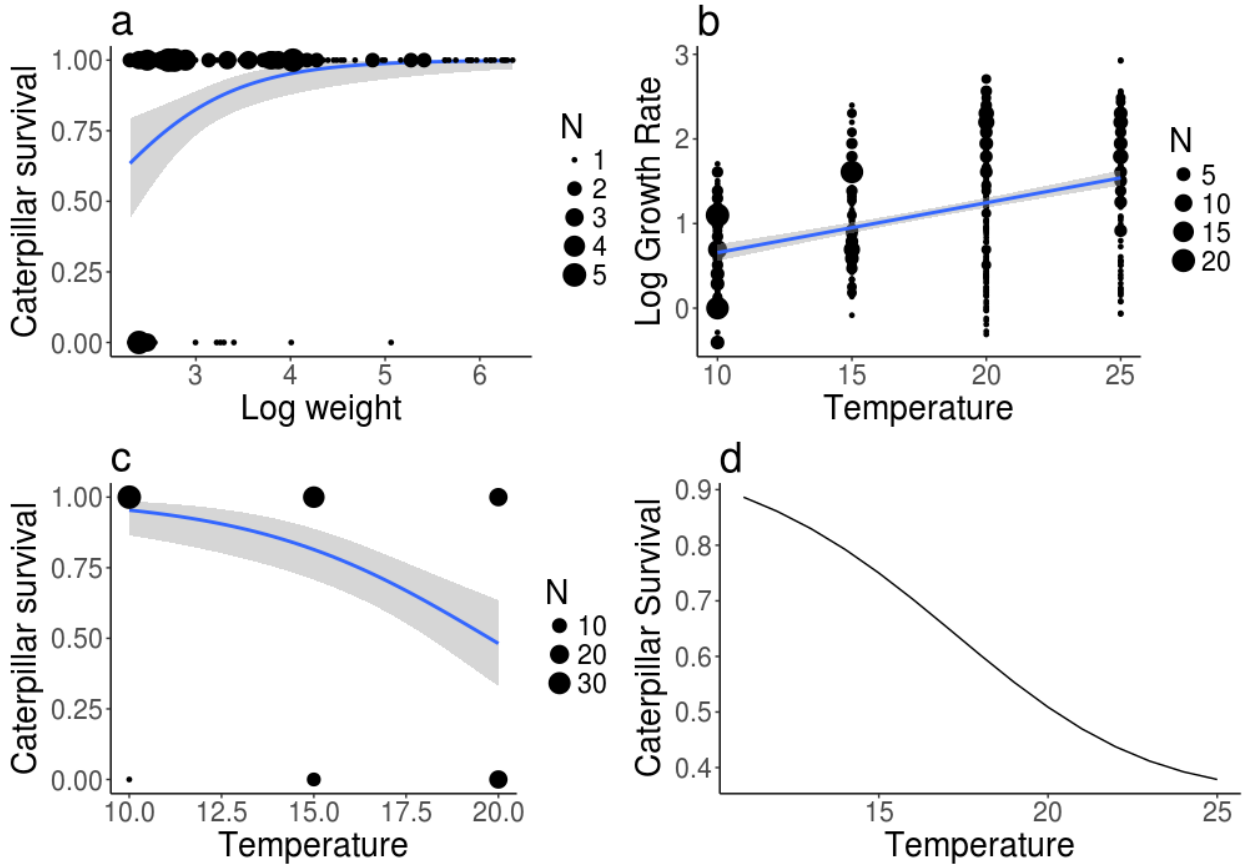

Figure 2.2. (a) Survival of caterpillars preyed upon by *F. lasioides* as a function of log caterpillar weight in the field with 95% confidence intervals. (b) Log growth rate of caterpillars by temperature with 95% confidence intervals. (c) Survival of caterpillars preyed upon by *F. lasioides* by temperature in the laboratory with 95% confidence intervals, from Karban et al. 2015. (d) Predicted survival probability of caterpillars by temperature from a model (equation 1) based on a combination of temperature-dependent growth rates, size-dependent predation rate, and temperature-dependent predation rate.

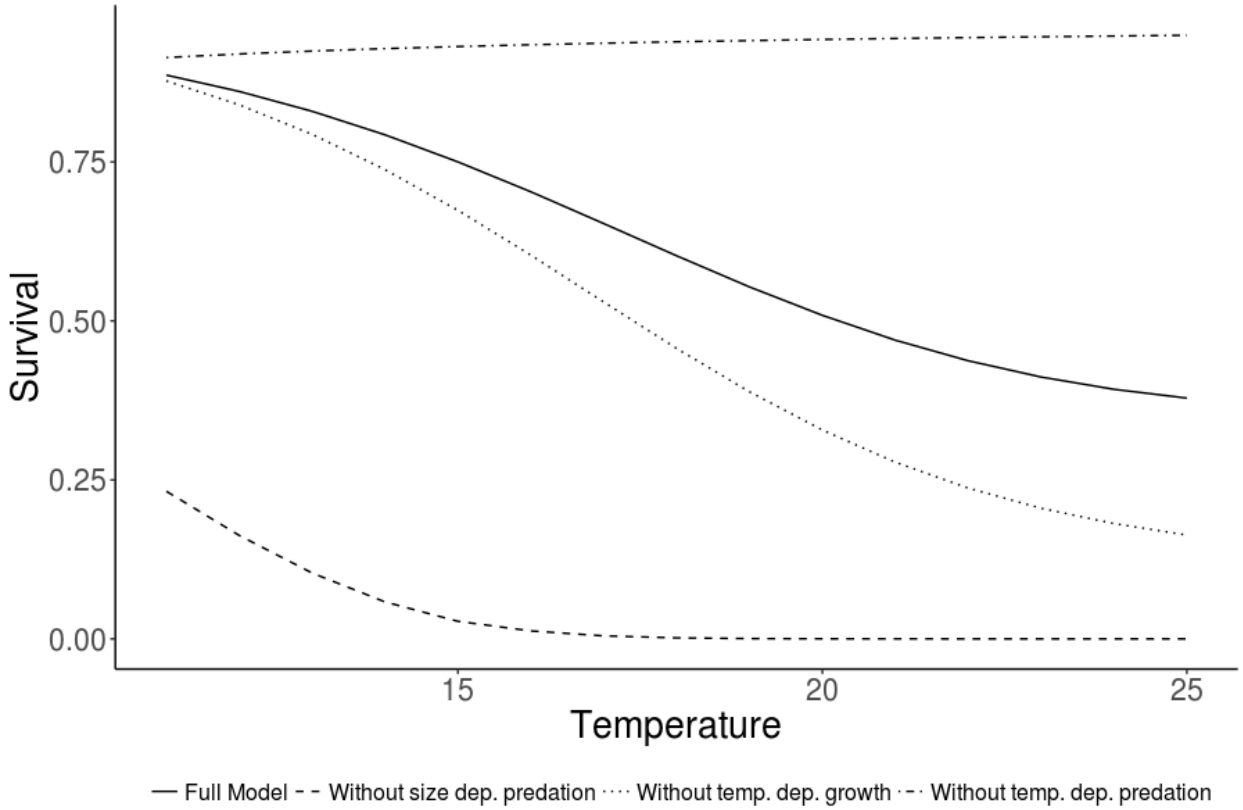

Figure 2.3. Sensitivity analysis of models of temperature-dependent caterpillar survival by removing parameters. Shown by line type is (1) the full model, (2) the model without size-dependent predation rate, (3) the model without temperature-dependent growth, and (4) the model without temperature-dependent predation.

3. Chapter II: Predator diversity and thermal niche complementarity attenuate indirect effects of warming on prey survival

As published in *The American Naturalist* with Marshall McMunn (Pepi and McMunn 2021)

3.1 Abstract

Climate warming has broad-reaching effects on communities. Although much research has focused on direct abiotic effects, indirect effects of warming mediated through biotic interactions can be of equal or greater magnitude. A body of theoretical and empirical work has developed examining the effects of climate warming on predator-prey interactions, but most studies have focused on single predator and prey species. We develop a model with multiple predator species using simulated and measured realized thermal niches from a community of ants, to examine the influence of predator diversity and other community thermal traits on the indirect effects of climate warming on prey survival probability. We find that predator diversity attenuates the indirect effect of climate warming on prey survival probability, and that sufficient variation of predator thermal optima, closer prey and mean predator thermal optima, and higher predator niche complementarity increases the attenuation effect of predator diversity. We predict therefore that more diverse and complementary communities are likely more affected by direct versus indirect effects of climate warming, and vice versa for less diverse and complementary communities. If general, these predictions could lessen the difficulty of predicting the effects of climate warming on a focal species of interest.

3.2 Introduction

Understanding the effects of climate drivers on population dynamics has become an important goal in ecological research, with the ultimate aim of predicting the effects of climate

change on communities and ecosystems (Walther et al. 2002, Parmesan 2006). A main driver of climate effects on population dynamics is warming, which affects ectotherms primarily through increased metabolic rate (Uszko et al. 2017). The direct effects of increased metabolic rates on ectotherms are complex and depend on details of life history, but some predictions are possible based on sufficient life history information (e.g., Bale et al. 2002; Deutsch et al. 2018). However, the effects of climate change on ecological communities is complicated by biotic interactions, and many effects of climate change on population and community dynamics are likely to be indirect and mediated through biotic interactions (Tylianakis et al. 2008, Post 2013), which cannot be predicted based solely upon the life-history of the focal species. This complexity makes predicting the impacts of climate warming on individual species, let alone whole communities, extremely difficult.

Recognizing the importance of biotic interactions as mediators of climate change effects, some research has investigated which factors influence climate effects on interactions. For example, mechanistic models and experimental work suggest that the equilibrium population size of predators and prey with warming can be predicted based on predator foraging mode and asymmetries in the relative response rates of predator and prey movement velocity to environmental temperature (Dell et al. 2014, Ohlund et al. 2014). Other work suggests that asymmetries in relative response rates of predator attack rate and development rates of prey with size- or stage-dependent refuges will also affect equilibrium population sizes (Culler et al. 2015, Pepi et al. 2018).

Thus far, most research has focused on single predator-prey pairs. However, most prey species likely interact with multiple predators, all of which will be affected by a warming climate in ways that vary with species' life histories (Barton and Schmitz 2009). Predator diversity is

likely to have important impacts on how climate warming affects prey population size, due to the compensatory effects on many trophic links. These compensatory effects might arise due to variation in predator thermal niches (*i.e.,* range of environmental temperatures utilized within a habitat) that are complementary with respect to foraging activity or fitness in a given range of temperatures (*i.e.,* low thermal niche overlap). In this situation, the change in maximum metabolic rate and thus potential attack rate (Vucic-Pestic et al. 2011, Karban et al. 2015) in response to environmental temperature by one predator might be concurrent with changes in another predator that may compensate for the change in attack rate by the first. Alternatively, variation in predator thermal niches may not result in compensation if thermal niches are similar (*i.e*., a large overlap): with very similar thermal niches, effects of warming on predation might be even more intense than expected for a single predator-prey pair, as attack rates for both predators increase or decrease together with temperature. Besides thermal optima and niche breadth, variation in thermal sensitivity of predators and skewness of thermal response curves may affect the likelihood of compensation across temperature to occur. In particular, significant variation in thermal sensitivity is likely to reduce this compensation effect because predators of significantly different thermal sensitivity will not create effective functional redundancy across temperature.

How warming will affect predator-prey interactions considering multiple predators likely depends on the community distribution of thermal response curves, or the community thermal niche (Kühsel and Blüthgen 2015). However, there has been very limited empirical work in this area. Kühsel and Blüthgen (2015) examined flower visitation rates by pollinators in agricultural meadows, and characterized the realized thermal niche of 511 species of arthropods based on activity rates across a range of temperatures, finding that higher thermal niche complementarity within communities resulted in greater predicted resilience of pollination function with warming.

Systematic variation by insect order was observed, with a great degree of variability of realized thermal niches across species within each community (s.d. of activity thermal optimum from 3.1-5.9°C in different taxa). There was also variation between communities in thermal niche complementarity, which was defined as a weighted coefficient of variation of thermal optima within the community.

For a community with substantial thermal niche variation, if prey species are consumed by multiple predators, it is likely that there will be both positive and negative asymmetries in thermal response rates between the prey species and predators (Figure 3.1). From this perspective, we can predict that thermal trait responses (e.g., growth rate) of a given prey species relative to all the thermal trait responses of the predators (e.g., attack rate) with which it interacts will determine whether climate effects mediated by predation lead to an increase or decline of the prey species. This means that for prey populations interacting with a single or few predator species it is very likely that asymmetries will be an important mediator of climate effects of population levels. However, as the number of interacting predator species increases, the likelihood that a large net asymmetry in thermal trait responses between predator and prey will remain becomes lower, if the predator thermal niches are not all warmer or cooler than the prey. In this latter situation, we would expect that the indirect climate effects mediated by biotic interactors become less important, and thus the direct effects of warming should be more important.

To investigate the effects of predator diversity on prey abundance due to thermal rate asymmetries in a warming environment, we developed a simulation model of predator-prey communities. For this study, we use the example of a univoltine invertebrate prey species with a temperature-dependent window of vulnerability, based on data from an Arctiine moth (*Arctia*

virginalis; Pepi et al. 2018). This type of life-history, in which a species is vulnerable to predators during a juvenile stage or below a certain size threshold that is approached at a temperature-dependent growth rate, is common across taxa (e.g., insects: Benrey and Denno 1997; amphibians: Werner 1986; marine organisms: Paine 1976, Mittelbach 1981, Christensen 1996). We used simulated communities of predators to test our prediction that increased predator diversity will weaken indirect effects of warming. We also characterized the realized thermal niches of a community of 23 species of ants in California as an empirical example of our simulated predator communities. We conducted sensitivity analyses to examine under which conditions we would expect predator diversity to attenuate the indirect effects of warming. We conducted sensitivity analyses on the range of variation (s.d.) of predator thermal optima, predator thermal niche breadth, the relative value of the predator community mean thermal optimum versus the prey species thermal optimum, and evenness of the predator species abundance distribution on changes to prey survival probability with warming.

3.3 Methods

Simulation model

We developed a demographic model to simulate temperature-dependent survival probability across one generation of a single prey species, interacting with one or many predator species, extending a model previously developed in Pepi et al. (2018). This model combines temperature-dependent growth of prey, prey size-dependent predation, and temperature-dependent attack of predators to simulate predation risk P at environmental temperature T :

$$P(T) = \prod_{i=1}^{m} logit^{-1}\, c\left\{a_0 + a\left(x_0^{r(T)t_i}\right)\right\} \sum_{j=1}^{n} \frac{r_j(T)}{n} \qquad (1)$$

in which t_i is time in days, m is the length of the simulation in days, x_0 is log initial caterpillar mass (10 mg), T is environmental temperature in Celsius (from 10-30 °C; chosen to correspond with empirical values below), r is instantaneous daily growth rate of the prey as a function of temperature, a_0 and a represent the intercept and slope of size-dependent daily predation, c is a constant to scale size-dependent predation at the starting size to 1, n is the number of predators species in the community, r_j is the daily predation rate of the predator j on prey as a function of temperature. To determine predation risk at each temperature, daily size-dependent predation risk is calculated based on prey size (scaled relative to a maximum predation rate of 1 at x_0), which in turn is calculated based upon temperature-dependent exponential growth. Size-dependent predation risk is multiplied by the combined (unweighted) average search and consumption (attack) rate of all predators in the community. The temperature-dependent growth rate (r) of prey and attack rate of predators (r_j) are modelled as unimodal Gaussian functions of environmental temperature (T) after Taylor (1981):

$$r(T) = r_{max} e^{-0.5\left(\frac{T-T_{opt}}{\sigma_{opt}}\right)^2} \quad (2)$$

in which r_{max} is the maximum rate, T_{opt} is the thermal optimum, and σ_{opt} determines the spread of the unimodal curve. For predators, the thermal optimum is drawn from normal distribution with mean μ and s.d. σ^2.

Simulations were conducted of predator communities including 1, 2, 3, 10, and 30 predators to assess the effects of predator diversity on prey under warming. Size-dependent predation risk was parameterized based on field data from *Arctia virginalis* caterpillars preyed upon by *Formica lasioides* (Pepi et al. 2018; Table 3.1). Temperature-dependent survival and

growth of *A. virginalis* caterpillars reared in incubators at constant temperatures from 10-25° C were estimated using equation 2 and used to compare the direct vs. indirect effects of warming (Pepi et al. 2018). A mean thermal optimum of 23.5 °C (to match the thermal optimum of *A. virginalis*; Table 3.1) was used for the distribution of the predator community, with a s.d. of 5, which is within the upper range of variation documented by Kühsel and Blüthgen (2015) in natural arthropod communities.

For each simulation, the indirect effect of warming on survival ($\Delta_{indirect}$) was calculated. We define this as the net change (positive and negative) in the difference between rearing survival and survival including rearing survival and predation risk with respect to environmental temperature T between minimum and maximum T. We calculate this value by integrating the absolute value of the derivative with respect to T:

$$\Delta_{indirect} = \int_{Tmax}^{Tmin} \left| \frac{d\{R(T) - R(T)P(T)\}}{dT} \right| dT \qquad (3)$$

in which $R(T)$ is rearing survival at temperature T, and $P(T)$ is predation risk at temperature T as defined in equation 1. We used the absolute value of the derivative because we are interested in how much net change is due to the indirect action of warming, in a positive or negative direction. According to the net change theorem and the definition of an absolute value, equation 3 simplifies to:

$$\int_a^b \left| \frac{d\{R(T) - R(T)P(T)\}}{dT} \right| dT$$

$$= \left| \big(\mathrm{R(a)} - \mathrm{R(a)P(a)}\big) - \big(\mathrm{R(b)} - \mathrm{R(b)P(b)}\big) \right|, \qquad (4)$$

$$for\ any\ monotonic\ interval\ a \to b$$

To identify sub-intervals that are monotonic we fit a third order polynomial function fit in the following form:

$$R(T) - R(T)P(T) \sim \alpha_0 + \beta_1 T + \beta_2 T^2 + \beta_3 T^3 \quad (5)$$

We then calculated all real roots of the derivative of this polynomial (5) to define monotonic sub-intervals. We calculated the absolute value of change within these sub-intervals as in equation 4, and summed all intervals for net change between minimum and maximum temperature. For each predator community size, 10,000 simulations were conducted and the distribution of $\Delta_{indirect}$ was summarized.

To test the broader applicability of the simulation model beyond the particular parameter values chosen for the initial constant parameter model, and to understand the broader ecological implications of the results, we conducted univariate sensitivity analyses. Model sensitivity to community thermal niche parameters was analyzed by individually varying the s.d. and mean of the distribution of predator thermal optima, and the spread of predator thermal niches (σ_{opt} in eq. 2). We conducted an additional sensitivity analysis of the main model assumption of a uniform predator species abundance distribution by using a lognormal species abundance distribution. For this sensitivity analysis, predator abundances were drawn from a distribution $N_j \sim Lognormal\ (1, \sigma^2)$, and converted to relative abundances out of the total number of species. This was calculated as a weight by dividing by the sum of species abundances and multiplying by the number of species ($w_j = \frac{n\, N_j}{\sum_{j=1}^{n} N_j}$). This resulted in a modification of equation 1 with a weighted average of predator attack rates:

$$P(T) = \prod_{i=1}^{m} logit^{-1}\, c\left\{a_0 + a\left(x_0^{r(T)t_i}\right)\right\} \frac{\sum_{j=1}^{n} r_j(T) w_j}{\sum_{j=1}^{n} w_j} \qquad (6)$$

Using this modification, σ^2 of the lognormal species abundance distribution was varied, starting at zero (which represents the base model assumption of even species abundances).

All simulations were conducted in R version 3.6.1 (R Development Core Team 2020), and plots were created using ggplot2 (Wickham 2016).

Empirical data: ant community thermal niche

Realized thermal niches of ants were estimated by pairing passively collected foraging ants with detailed ground surface temperature measurements. This results in a combined activity-abundance measure as a function of temperature, which should be proportional to prey encounter rate. Collections were made using automated time-sorting pitfall traps, which simultaneously measure ground-surface temperature and separate active ants into 24 separate hour-long pitfall samples (McMunn 2017). To install traps, we carefully removed leaf litter and dug a small hole approximately 20 cm wide, 30 cm long, and 20 cm deep. We then buried the trap; replacing soil flush with the top the trap entrance, a funnel coated with fluon (Insect-a-slip, Bioquip, Rancho Cordova, CA). We replaced leaf litter, taking care to minimize the disturbance to the surrounding litter and soil. After installation, the traps remained closed to ants for 24 hours to avoid ants being initially attracted to the soil disturbance following pitfall trap installation (Greenslade 1973). We separated ants from all other collected arthropods, identified each individual to species, and after confirmation of species identifications by Philip Ward (UC Davis), deposited vouchers at the Bohart Museum of Entomology (UC Davis).

The study area consisted of 4.2 hectares of mixed sagebrush shrubs and coniferous forest in the Sierra Nevada mountain range (2000 m, 39.435583°N, 120.264017° W). The range of *A. virginalis*, which was used to parameterize the prey thermal response in the simulation model,

extends to this geographic area. Of the ant species in this community with known diets, all are omnivorous and would consume lepidopteran larvae if encountered, though we have directly observed predation of *A. virginalis* by only two species (*Formica lasioides* and *Tapinoma sessile)*. We made collections between 19 June and 14 October 2015, concentrated in one- or two-week sampling bouts each month. From a grid of 600 potential sites across the habitat, we randomly selected 127 sites for 24 hourly ant collections. Over the season, this resulted in 3048 hour-long samples of ant abundance (24 hrs × 127 sites = 3048 hourly samples). The traps recorded temperature measurements every 5 minutes using a K-type thermocouple datalogger at a height of 1-3 mm above the surface of the leaf litter or above the surface of the soil if no litter was present (McMunn 2017). We took the mean of all temperature measurements within the 1-hour ant collection windows and used this hourly mean to estimate ant thermal niche. In general, ant body temperature rapidly equilibrates to environmental temperature due to small body size (Kaspari et al. 2015), so we assumed that ants captured at a given temperature likely experience a body temperature similar to temperature measured on our thermocouples.

Ant realized thermal niche was modelled by species with equation (2) fit using nls (package nlme, Pinheiro et al. 2017), using abundance data aggregated across all sampling locations and dates.

We expected ant occurrence and abundance to be strongly affected by factors other than temperature (e.g., leaf litter depth, time of day) and suspect many of these factors contributed to the broad and overlapping realized thermal niches we observed. Realized thermal niche provides estimates of the effects of temperature on ant activity within a natural community and provide a conservative estimate of the attenuation effect of predator diversity on indirect effects of warming. Fitted parameter values for 23 ant species that were sufficiently abundant to

successfully fit thermal response curves were used to generate simulated communities of varying diversity. Species were drawn randomly without replacement from this set of 23 for simulations, using the same procedure as described above, except that values of T_{opt} and σ_{opt} were fitted values from the ant community data. We did not account for predator body size in this updated model (or in the original), as nearly all ants were a similar magnitude smaller than prey species (roughly 1/10 the size of caterpillars or less). Since there were large differences in abundance between ant species in this community (which is dominated by 2-3 species), simulations were conducted both with estimated r_{max} values (maximum activity rate by species), and with all values of $r_{max} = 0.8$, to create an even distribution of species. Although this adjustment does not represent the likely effect of actual warming in this specific community, we set abundances to be even to estimate the maximal effect of varying degrees of diversity using thermal traits of a real assemblage of species, since this community had a very low effective diversity due to strong dominance and low evenness.

3.4 Results

Individual simulations generally showed more stability in overall predation rate over the environmental temperature range with higher predator diversity (Figure 3.2), and the results of many simulations together showed a decrease in $\Delta_{indirect}$ with higher predator diversity (Figure 3.3a) with the initial constant parameter values (Table 3.1). In simulations using empirical ant community data, greater ant diversity did not generate a decrease in $\Delta_{indirect}$ with fitted r_{max} values (Figure 3.3b), but with all values of $r_{max} = 0.8$, greater ant diversity did lead to a decrease in $\Delta_{indirect}$(Figure 3.3c).

Increasing the s.d of predator thermal optima increased the effect of diversity on $\Delta_{indirect}$ up to an s.d. of ~8 (Figure 3.4b), and changing the mean of predator thermal optima increased

the effect of diversity of $\Delta_{indirect}$ when the mean was closer to the prey thermal optimum in terms of survival (17.66 °C ; Figure 3.4a). Increasing the breadth of predator thermal niches decreased the effect of diversity on $\Delta_{indirect}$ (Figure 3.4c). Increasing variation in relative species abundances increased the number of species required to reduce $\Delta_{indirect}$(Figure 3.4d).

3.5 Discussion

We show in our simulations, using simulated and fitted parameter values from a predator-prey community of ants and a caterpillar, that increasing predator diversity may under some circumstances attenuate indirect effects of warming on prey species. The attenuation of the indirect effects of warming we define here as the change in survival probability due to changing interactions with predators ($\Delta_{indirect}$). The vast majority of the attenuation effect of diversity results from very small increases in diversity in most cases (Figures 3.3, 3.4), because having even two vs. one species greatly reduces the likelihood of thermal asymmetries in simulated communities. We find the attenuation effect of diversity is greater when there is sufficient variation in predator thermal optimum and when predators have narrower, non-overlapping niches: that is, when predators have higher thermal niche complementarity. The effect of diversity on $\Delta_{indirect}$ is greater when the mean of the distribution of predator thermal optima is closer to the thermal optimum of prey survival. In addition, effect of diversity on $\Delta_{indirect}$ is greater when relative predator species abundance is close to even. Overall, this suggests that higher effective predator diversity and thermal niche complementarity may buffer indirect effects of warming on a prey species. Our findings also predict that in general, climate warming effects on prey species that are preyed upon by many thermally complementary predator species (i.e., with non-overlapping niches) should primarily be direct as opposed to indirect effects. If generally applicable, this prediction could aid in distinguishing in which circumstances direct

effects of warming, which have the potential to be predictable based on species life-history information, are likely to dominate vs. those in which indirect effects of warming would be expected to dominate. This would have the potential for significant value in unravelling some of the complexity of the effects of climate on species when considering trophic interactions (e.g., Post 2013; Dell et al. 2014).

In addition to purely simulated communities of predators, we parameterized our simulation model using empirical data from a community of ants. In this case, rather than using measured attack rates, we use ant activity-abundance rates at a given temperature, which is likely to be proportional to attack rate on prey at a given temperature. In general, we expect attack rate to be proportional to search or discovery rate which generally increases with temperature up to the thermal optimum of ants (Prather et al. 2018). Due to extreme variation in the rank abundances of ants (see Table 3.2), we found no effect of diversity on $\Delta_{indirect}$ with fitted r_{max} values; however there was an effect of diversity when all r_{max} values were set to be the same. We set all r_{max} values as equal because we were interested in examining the effect of varying levels of effective predator diversity using a real assemblage of species; using fitted r_{max} values amounted to imposing a very low maximum diversity due to high dominance. The effect observed with equal r_{max} values from the ant community was smaller than that of simulations using purely simulated parameter values because this community of ants consists largely of thermal generalists that have large niche breadths (σ_{opt}) relative to the variation of thermal optima (T_{opt}) and low complementarity (i.e., large niche overlap; Figure 3.5). The fact the we observed an effect of predator diversity on $\Delta_{indirect}$ (albeit with adjusted r_{max} values) even in a predator community that our *a priori* expectation would be for little or no effect of diversity lends credence to the idea that this effect may be common in nature, in communities with similar

or higher thermal niche complementarity. In addition, since our measured community includes only species from the same family (Formicidae), it is likely a significant underestimate of the thermal niche diversity in the full community of arthropods at this site, which includes taxa with generally very different thermal niches than ants (e.g., hemipterans, spiders, solifugids, etc.).

In this study we emphasize the concept of the community thermal niche, first developed by Kühsel and Blüthgen (2015), which refers to the collection of the thermal niches of all the individual species in the community. In light of what we have shown in our simulations, we believe that the community thermal niche is a valuable concept to help understand how communities are likely to respond to climate warming, and that a collection of such community datasets would significantly advance our understanding of the ecological effects of warming. There has been a great deal of both empirical (e.g., Brown et al. 2004; Kingsolver and Huey 2008; Kingsolver 2009; Dell et al. 2011) and theoretical work (e.g., Rall et al. 2010; Dell et al. 2014; Uszko et al. 2017) on the effects of temperature on fitness, species interactions, and even simple food webs (Petchey et al. 1999, 2010, Barton and Schmitz 2009). However, the extension of thermal ecology to thermal community ecology should be a priority since individual species and species interactions exist within broader food webs and ecological communities. With the theoretical perspective developed here, some predictions can be made about which aspects of community thermal niche might be important for outcomes with a warming climate.

The range of variation of thermal optima in a community is the primary aspect of the community thermal niche that we expect to mediate effects of warming on a community. As identified by Kühsel and Blüthgen (2015), greater variation in thermal optima in a community represents higher functional diversity, which has been predicted by theory to create greater resilience to environmental change, which they found to be the case for the communities of

pollinators that they studied. In the present study, we show further that large variation of thermal optima in a community increases the potential for predator diversity to attenuate indirect effects of warming on prey species. This has the potential to aid in predictions of the effects of warming on predator-prey dynamics: if a community has sufficient variation in predator thermal niches, then we can expect that climate will have a greater effect on prey species via direct effects than indirect effects.

The breadth of thermal niches within a community is another aspect of the community thermal niche that we expect to have important implications for the effects of warming on a community. For community resilience, greater thermal niche breadth has a positive effect, since greater breadth of function can only increase resilience (Kühsel and Blüthgen 2015). Kühsel and Blüthgen (2015) define thermal niche complementarity for their purposes as the weighted coefficient of variation of thermal optima. Since we are interested in the degree of change in predation risk with temperature, complementarity here results from a combination of sufficient variation in predator thermal optima as well as narrower predator niche breadth (Figure 3.4b-c). Narrower thermal niches with sufficiently different optima result in less change in predation risk with environmental temperature because as one predator becomes less active, there is another that is becoming more active, resulting in a consistent predation risk despite changing temperature. In this way, high complementarity combined with greater species diversity should lead to much weaker indirect effects of warming.

From here, we can ask in which communities do we expect to see narrower thermal niches, greater variation in thermal optima, and greater diversity of predators, and therefore weaker indirect effects of warming? Generally, we expect to see narrower thermal niches (Janzen 1967, Deutsch et al. 2008) and greater diversity (Mittelbach et al. 2007) of ectotherms in the

tropics. All else being equal this would predict weaker indirect effects of warming in the tropics. However, if ectotherms in temperate environments have higher variation in thermal optima than in the tropics, this might counteract broader niches in the temperate zone in terms of the attenuation effect of predator diversity on indirect effects of warming. In this scenario, whether temperate and tropical ectotherm predator communities have similar or different thermal niche complementarity might depend on if the relative magnitude in the increase of niche breadth and variation in thermal optima with latitude are similar or different enough to result positive, negative, or no change in complementarity with latitude.

We also found from sensitivity analyses that decreasing distance of the thermal optimum of prey survival (in our simulations, 17.66 °C) from the mean of predator thermal optima both leads to greater overall indirect effects of warming and greater attenuation of indirect effects by predator diversity. This means that the thermal optimum of a prey species relative to the community of potential predators has important implications with respect to climate warming effects. If we assume that a species has an invariant thermal niche across its range (which may or may not be the case; Angilletta Jr et al. 2002), and that most species are best adapted to thermal conditions at the climatic mean of their range, then on average a species near its range limit is likely to have a lower thermal optimum than most other species in the community at the warmer edge, and a higher thermal optimum than most other species at the colder range edge. If this is the case we can expect much stronger indirect effects of warming at range edges, due to more consistent directional asymmetries and therefore weaker compensating effects of predator diversity. Such effects could contribute to range shifts due to climate warming, through negative indirect effects at warmer range edges, and positive indirect effects at the colder range edge.

Our modelling approach makes several simplifying assumptions. First, we examine only short-term dynamics, consider only prey survival and reproduction, and do not consider long-term outcomes. This is because coexistence of multiple predators in the long term is not simple, since generally whichever predator more efficiently utilizes a prey species will outcompete all the others (Tilman 1982), and examining mechanisms of predator coexistence is beyond the scope of this study. In addition, we do not consider the effects of warming on predator-predator interactions, nor of functional responses to prey density. The effect of predator-predator interactions are likely to result in dominance of some predators over others, which based on our results would be expected to reduce the attenuating effect of predator diversity on indirect effects of warming. Similarly, if predators differ in their functional responses to prey density as it decreases over time (e.g., prey-switching or not), that would likely serve to reduce the attenuating effect of predator diversity. In both cases, greater predator diversity would likely be required for an equivalent attenuating effect.

Based on our results, we see several further theoretical and empirical research directions that we believe would provide significant insight into the topic of predicting indirect vs. direct effects of climate warming on predator-prey communities. Further modelling work could incorporate short-term dynamics as explored here into dynamical models examining long-term behavior of predator-prey communities with varying traits that influence significant aspects of the community thermal niche. In addition, further modelling work could investigate the effects of multiple prey species and integrate effects of the community thermal niche and food web structure. The empirical characterization of the community thermal niche of more species assemblages is also an essential next step to further test ideas developed here. We believe that these data are essential for understanding how climate warming will affect communities through

direct vs. indirect pathways. Automated sampling methods as used here (McMunn 2017) offer the potential to relatively easily characterize the thermal activity distributions of other assemblages of invertebrates, a task which would otherwise be logistically difficult. Lastly, manipulative experiments of warmed communities in mesocosms would offer the strongest test of hypotheses developed here with regard to how multiple aspects of the community thermal niche will influence the relative importance of direct vs. indirect effects of warming on predator-prey communities.

3.6 Conclusions

Theoretical and empirical work investigating the effects of climate warming on species interactions has made significant progress in describing how climate warming is expected to affect ectotherm predator-prey pairs (e.g., Dell et al. 2014; Uszko et al. 2017). Little work has extended to examine the effects of warming on multi-species interactions (but see Barton and Schmitz 2009). We propose that the community thermal niche (Kühsel and Blüthgen 2015) is a useful concept and approach to investigate community dynamics under climate warming, based on predictions with regard to community thermal niche traits from our simulation models developed here. Specifically, we predict that species preyed upon by many thermal complementary predators will experience weaker indirect effects of warming than those that are preyed on by fewer or less complementary predators. Predictions that can be derived from traits of species composing a community are essential if we are to decompose some of the complexity of climate warming effects on communities that are mediated through biotic interactions (cf. Tylianakis et al. 2008; Post 2013; Dell et al. 2014).

3.7 Acknowledgements

We would like to thank Jay Rosenheim, Marcel Holyoak, and Richard Karban for help improving our manuscript, and Philip Ward for assistance in identifying ant specimens.

3.8 Tables & Figures

Parameter	Description	Value when constant	Source
Size-dependent predation:			
a_0	Intercept	2.7576	Pepi et al, 2018
a	Slope	-1.438	
x_0	Starting size	10 mg	
c	Scaling constant	2.739361	
Prey growth:			
r_{max}	Maximum rate	5.9	Fitted from rearing data in Pepi et al. 2018.
T_{opt}	Thermal optimum	23.5℃	
σ_{opt}	Niche breadth	6.7℃	
Prey rearing survival:			Estimated from unpublished data: rearing method in Pepi et al. 2018.
r_{max}	Maximum rate	0.75299	
T_{opt}	Thermal optimum	17.661℃	
σ_{opt}	Niche breadth	7.9℃	
Predator attack rate:			
r_{max}	Maximum rate	0.8	r_{max} extrapolated from data in Karban et al. 2015, $\mu\ of\ T_{opt}$ set equal to T_{opt} of prey, $\sigma\ of\ T_{opt}$ and σ_{opt} chosen based on values in Kühsel and Blüthgen 2015.
$\mu\ of\ T_{opt}$	Mean of thermal optimum	23.5℃	
$\sigma\ of\ T_{opt}$	Standard deviation of thermal optimum	5℃	
σ_{opt}	Niche breadth	4℃	

Table 3.1. Values of parameters used for simulations, or values when parameters were held constant in sensitivity analyses.

Species	Frequency
Formica lasiodes	1639
Formica fusca	1182
Formica argentea	334
Formica sibylla	220
Camponotus modoc	197
Formica neoclara	150
Formica accrete	123
Manica invidia	122
Temnothorax nevadensis	115
Myrmica tahoensis	82
Temnothorax rugatulus	70
Formica obscuripes	68
Tapinoma sessile	68
Temnothorax nitens	48
Formica ravida	44
Formica sp. c.f. sibylla	28
Camponotus vicinus	14
Stenamma smithii	13
Aphaenogaster occidentalis	6
Myrmica discontinua	5
Camponotus laevissimus	4
Leptothorax muscorum complex	3
Camponotus essigi	1

Table 3.2. Ranked frequency of ant species in collections, across all times and sampling locations.

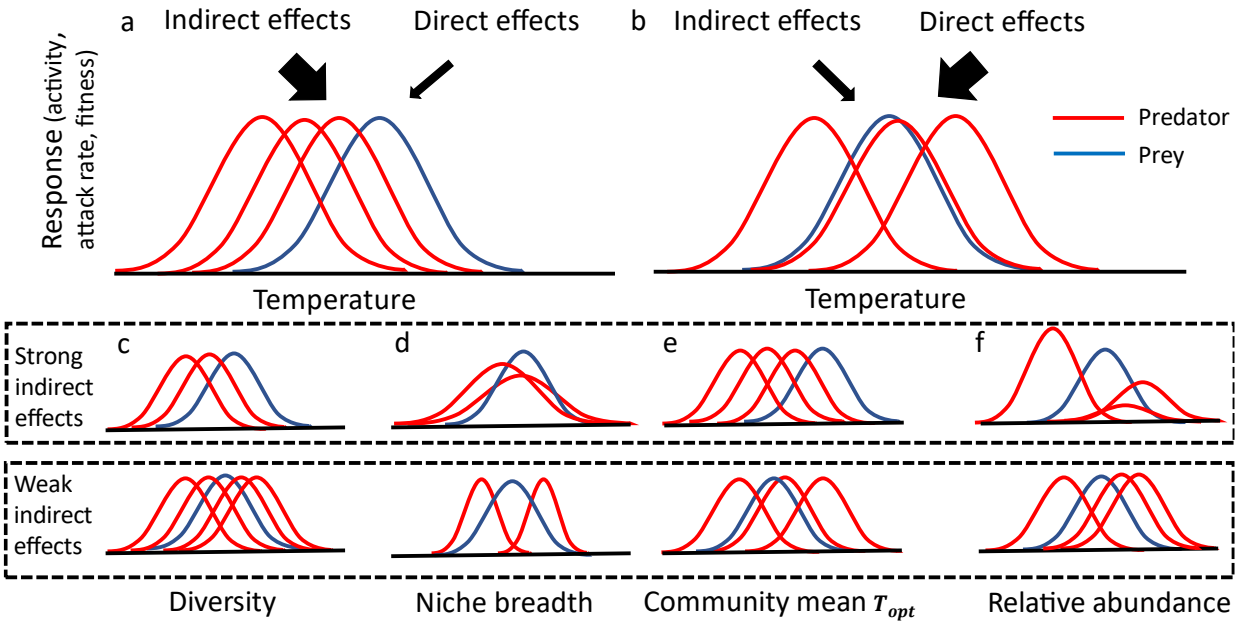

Figure 3.1. Schematic diagram of community traits that influence the relative importance of direct vs. indirect effects of warming on interactions between a prey species (blue) and a community of predators (red). Large asymmetries in thermal niches between predators and prey will result in large indirect vs. direct effects of warming (a), whereas symmetric thermal niches will result in larger direct vs. indirect effects (b). Asymmetries in thermal responses between prey and the predator community and thus the relative magnitude of indirect vs. direct effects depend on multiple aspects of the predator community thermal niche. Based on our simulation models, we hypothesize that (c) greater diversity, (d) narrower thermal niche breadth, (e) correspondence between the community mean thermal optimum and prey thermal optimum, (f) an even predator species abundance distribution, and greater community variation in species thermal optima (not shown) will result in weaker indirect effects vs direct effects of warming. The top row of (c-f) represents scenarios in which strong indirect effects are expected, vs the bottom row of (c-f) in which weak indirect effects are expected.

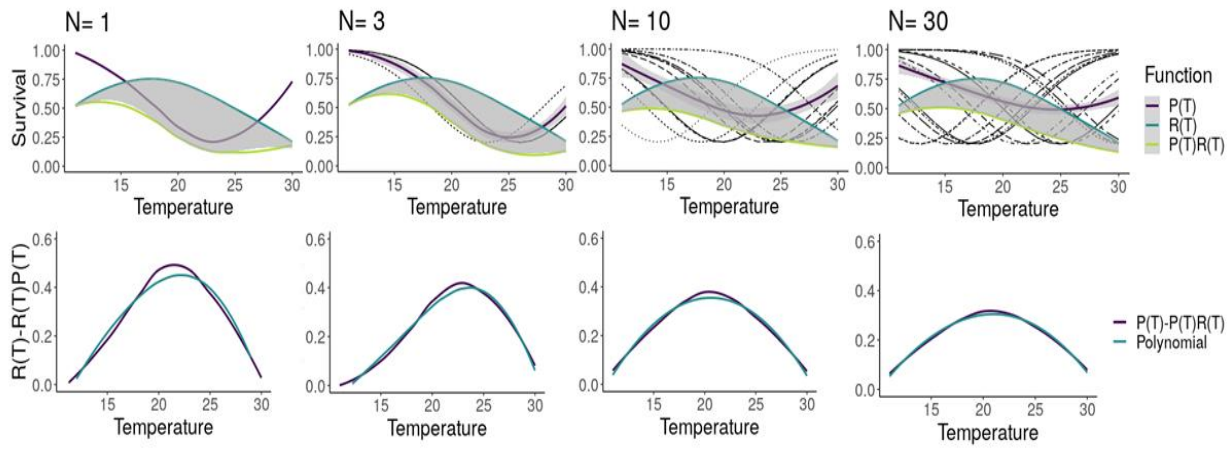

Figure 3.2. Representative simulation results of prey survival with increasing temperature preyed upon by 1-30 predator species, from left to right, showing reduced indirect effects of warming with increasing diversity. In the first row, black lines show (1 - predation rate) of each predator (not visible for N=1), with additional lines showing P(T) (1- mean predation rate, eq. 1) of all predators with a 95% CI, rearing survival of prey [R(T), eq. 2], and the combined effects of predation and rearing on survival [R(T)P(T)]. The grey band in the first row shows the indirect effect of warming on survival [R(T)-R(T)P(T)]. In the second row, the indirect effect of warming [R(T)-R(T)P(T)] is shown along with the fitted cubic polynomial (eq. 5).

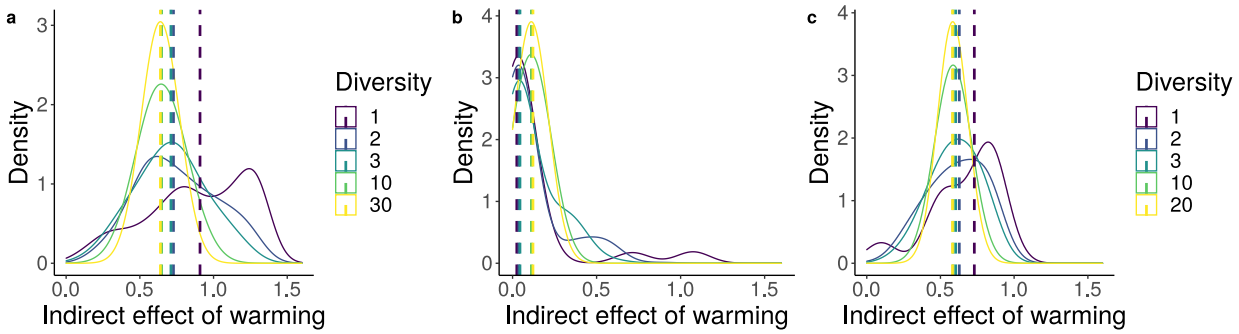

Figure 3.3. Distribution of indirect effects of warming from 10,000 simulations of a prey species preyed upon by a community of 1-30 predators, with (a) a simulated community of predators (b) a community of ants in California and (c) the same community of ants with $r_{max} = 0.8$ for all species. The median of each distribution is displayed by a dashed vertical line.

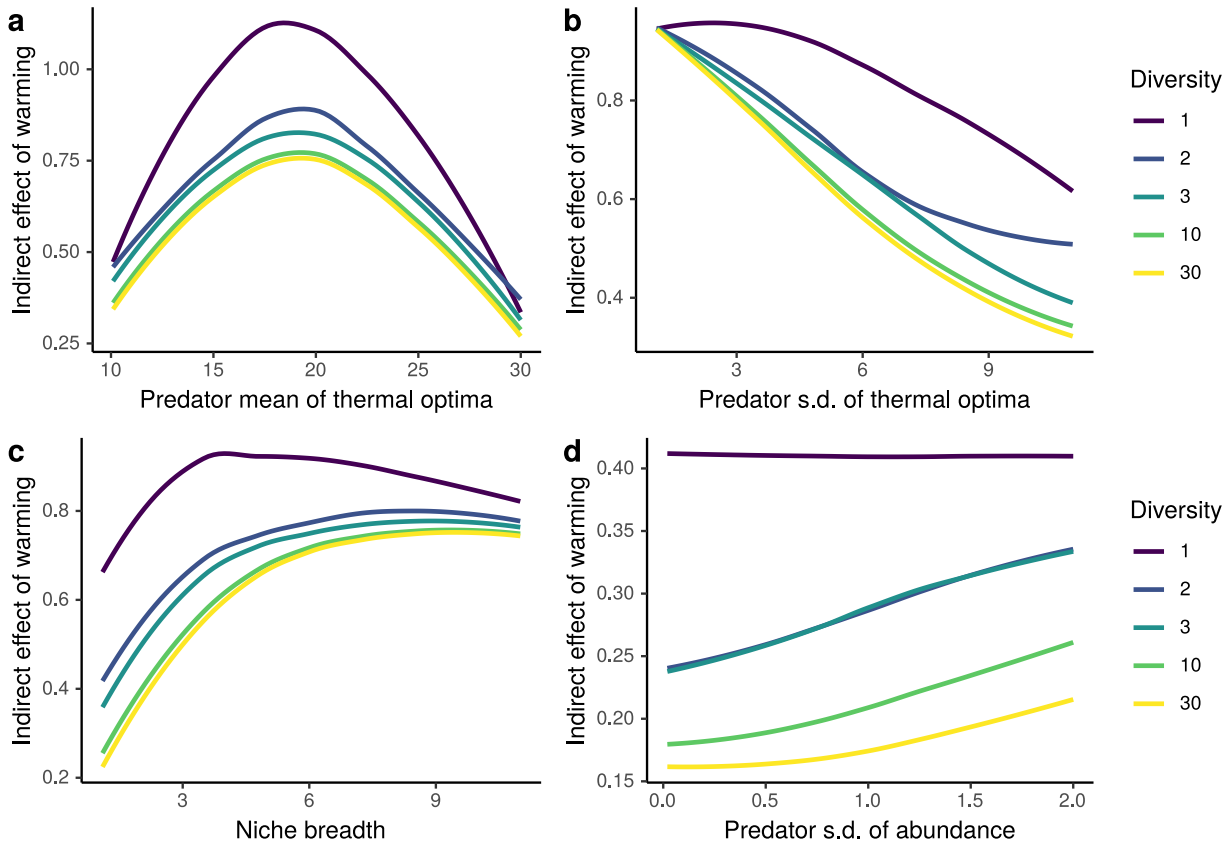

Figure 3.4. Sensitivity analysis of simulation model, showing the median indirect effect of warming ($\Delta_{indirect}$) for communities of 1, 2, 3, 10 and 30 predators. Sensitivity analyses are shown with respect to (a)mean of predator thermal optima (T_{opt}), (b) standard deviation (s.d.) of predator thermal optima , (c) predator thermal niche breath (σ_{opt}), and (d) s.d. of the lognormal species abundance distribution.

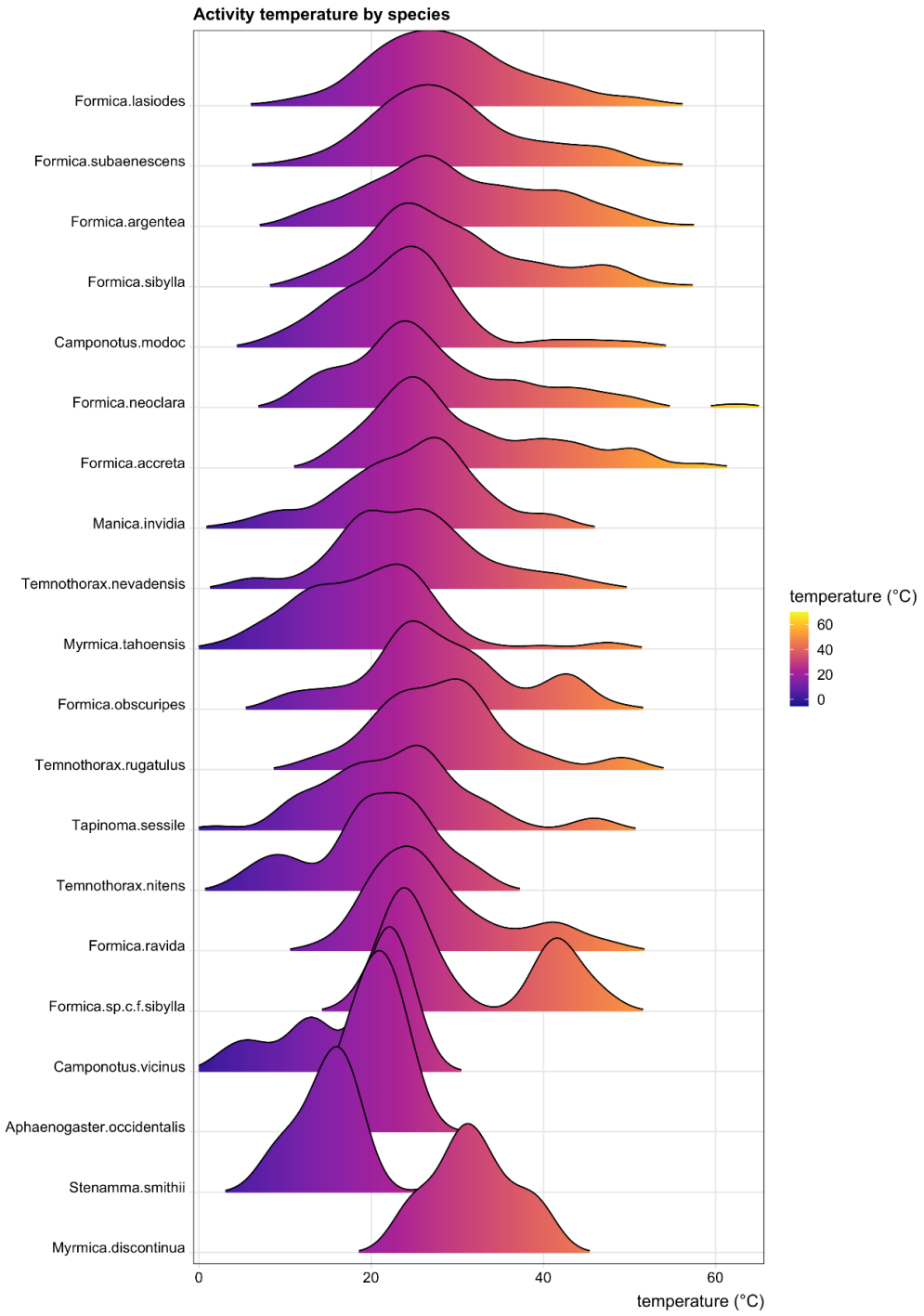

Figure 3.5. Density plot of ant activity by temperature and species. Species are ordered by rank abundance, from most abundant at the top to least abundant at the bottom.

4. Chapter III: Influence of delayed density and ultraviolet radiation on caterpillar granulovirus infection and mortality

(With Vincent Pan and Richard Karban)

4.1 Abstract

1. Infectious disease is an important potential driver of population cycles, but this must occur through delayed density-dependent infection and resulting fitness effects. Delayed density-dependent infection by baculoviruses can be caused by environmental persistence of viral occlusion bodies, which can be influenced by environmental factors. In particular, ultraviolet radiation is potentially important in reducing the environmental persistence of viruses by inactivating viral occlusion bodies.
2. Delayed density-dependent viral infection has rarely been observed empirically at the population level although theory predicts that it is necessary for these pathogens to drive population cycles. Similarly, field studies have not examined the potential effects of ultraviolet radiation on viral infection rates in natural animal populations. We tested whether viral infection is delayed density-dependent with the potential to drive cyclic dynamics and whether ultraviolet radiation influences viral infection.
3. We censused 18 moth populations across nearly 9° of latitude over two years and quantified the effects of direct and delayed density dependence and ultraviolet radiation on granulovirus infection rate, infection severity, and survival to adulthood. Caterpillars were collected from each population in the field and reared in the laboratory.
4. We found that infection rate, infection severity, and survival to adulthood exhibited delayed density dependence. Ultraviolet radiation in the previous summer decreased infection severity, and increased survival probability of the virus. Structural equation

modelling revealed that the effect of lagged density on moth survival was mediated through infection rate and infection severity, and was 2.5-fold stronger than the effect of ultraviolet radiation on survival through infection severity.

5. Our findings provide clear evidence that delayed density dependence can arise through viral infection rate and severity in insects, which supports the role of viral disease as a potential mechanism, among others, that may drive insect population cycles. Furthermore, our findings support predictions that ultraviolet radiation can modify viral disease dynamics in insect populations, most likely through attenuating viral persistence in the environment.

4.2 Introduction

Infectious disease plays an important role in population dynamics, potentially regulating populations and driving cycles. Many insect populations undergo dramatic cyclic fluctuations, and periodic delayed density-dependent disease outbreaks have been proposed as an explanation (Anderson and May 1980, 1981). However, many other mechanisms have also been proposed to explain insect population cycles (Myers and Cory 2013), particularly specialist parasitoids (Berryman 1996). For some species of Lepidoptera, empirical evidence has suggested that baculoviruses are most likely the cause of cyclicity (Myers 2000, Myers and Cory 2013, 2016), though this has not been formally tested.

Delayed density-dependent feedbacks are required to drive cyclic population dynamics (May 1973, Turchin 2003). Detection of delayed density-dependence involving many ecological factors has been common (Turchin 1990), and there have been several observations that viral epizootics follow high densities of some insect species (Myers 2000, Cory and Myers 2003, Fuxa 2004, Myers and Cory 2016). However, direct demonstrations of delayed density-dependent

viral infection rate and infection-induced mortality are less common (Fleming et al. 1986, Rothman 1997, Burthe et al. 2006). Observational studies over relatively small areas (>15km) using space-for-time substitutions of local densities have shown delayed density-dependent incidence of viral infection in voles (Burthe et al. 2006) and soil-dwelling hepialid caterpillars (Fleming et al. 1986). Experimental manipulation of western tent caterpillar (*Malacosoma californicum pluviale*) densities at the tree level showed delayed density-dependent infection rates by a nucleopolyhedrovirus (Rothman 1997).

Besides host density, other aspects of the local environment may affect viral transmission and dynamics in the field (Cory and Myers 2003). In particular, ultraviolet radiation has been shown to inactivate viruses of all kinds (Sagripanti and Lytle 2007), including baculovirus occlusion bodies (Witt and Stairs 1975, Griego et al. 1985). In field studies, examination of the presence of baculovirus occlusion bodies on shaded vs. unshaded foliage suggested that sunlight on leaves may inactivate viruses (Olofsson 1988). A study of baculovirus transmission in forest tent caterpillars (*Malacosoma disstria*) found depressed transmission rates on forest edges as opposed to the forest interior, which was attributed to sunlight inactivating virus on leaves at forest edges (Roland and Kaupp 1995). A field study of two strains of gypsy moth NPV showed variable resistance of virus to ultraviolet, in which inactivation rate from ambient ultraviolet was greater in a more potent strain than a less potent one (Akhanaev et al. 2017). In another study of forest tent caterpillars using tree ring analyses, it was suggested periods of weaker ultraviolet radiation increased the effect of forest tent caterpillar outbreaks on tree growth (Haynes et al. 2018). In this example, less ultraviolet radiation may have allowed better viral persistence and transmission and produced more severe caterpillar outbreaks.

In the present study, we examined the effects of host density, delayed-density dependence, and ultraviolet radiation on the survival, infection rate, and infection severity of an undescribed granulovirus (see supplement) in Ranchman's tiger moth (*Arctia virginalis*). Ranchman's tiger moth (Erebidae:Arctiinae) is a univoltine species with a long larval stage – usually lasting from late summer until the following spring. Pupation occurs in late spring, and adults emerge in early summer, mate and lay eggs during the summer. Larvae hatch mid-summer, and feed cryptically in litter and undergrowth until they become larger in winter months. Caterpillars are generalists and feed on a variety of herbaceous plants, with a preference for alkaloid-containing hosts (Karban et al. 2010), and occur mostly in open grassland, shrubland, or savannah. Caterpillars are parasitized by tachinid parasitoids, though caterpillars sometimes survive parasitism (English-Loeb et al. 1990). Parasitism has been found to have little role in population dynamics, leaving the observed oscillatory dynamics largely unexplained (Karban and de Valpine 2010). Caterpillars also sometimes show symptoms of granulovirus infection, which include poor growth, inactivity, watery, opaque frass, regurgitation of milky fluid, and death. Granulovirus is a dsDNA virus that persists outside of the host in the environment within a protective protein shell as an occlusion body (OB). Horizontal transmission can occur when caterpillars consume OBs on food sources, which dissolve in caterpillars' alkaline gut and release infective virus particles (Vega and Kaya 2012). Virus particles infect the caterpillar starting from the epithelial tissue and then move to other parts of the body, including the trachea, fat bodies, and hemolymph (Barrett et al. 1998), potentially causing death of the caterpillar. In Ranchman's tiger moth (*Arctia virginalis*), granulovirus, like parasitoids, does not uniformly kill its hosts.

To test the potential role of granulovirus in delayed-density dependent population dynamics in Ranchmans' tiger moth and the influence of ultraviolet radiation on the persistence and transmission of virus in moth populations, we censused 18 populations over two years along a gradient of latitude and ultraviolet radiation and reared caterpillars from these populations in the laboratory. To identify the mechanisms through which granulovirus affects moth population dynamics, we measured granulovirus infection rate, severity, and survival of caterpillars to adulthood. We analyzed the effect of caterpillar density and ultraviolet radiation at the study sites on viral infection and survival. We also tested whether viral infection mediated the effects of caterpillar density and ultraviolet radiation on caterpillar survival using a structural equation model.

4.3 Methods

Censuses

Caterpillars were counted visually along 4-m wide linear transects of varying length (78-300 m, depending on amount of habitat) at 18 sites along a ~1000 km latitudinal gradient of the Pacific coast in California, Oregon, and Washington (Figure 4.1). Transects were surveyed in 2019 and 2020, between 1 March and 30 May. We visited sites in each year from south to north, in accordance with the phenology of caterpillar development so that caterpillars were surveyed when most were 4^{th} or 5^{th} instars (sampling dates in Table 4.2). Transects were surveyed at a constant walking speed and all by the same observer (A. Pepi). Density was estimated from caterpillar counts over the transect area (4-m x length). During the second year, sites were revisited within 10 days from the calendar date of the first visit; however, this species is a slow-growing caterpillar (approximately 10 month development period; personal observation, Adam Pepi and Richard Karban), so density estimates were likely not overly sensitive to small

deviations in sampling date. In 2020, up to ca. 30 caterpillars per site were collected haphazardly and brought back to the laboratory for rearing.

Rearing

Caterpillars were reared individually in 180 ml plastic souffle cups with fabric lids and kept in an incubator at 18ºC and 75% relative humidity. Caterpillars were fed every 3-4 days with washed organic romaine lettuce and leaves of yellow bush lupine (*Lupinus arboreus*) collected from a part of Bodega Marine Reserve without *Arctia virginalis* (to avoid potential exposure to viral occlusion bodies on foliage). Parasitoids that emerged from caterpillars were counted and identified to family. Caterpillars that died during rearing were frozen at -20ºC for subsequent dissection, except for those that clearly died due to emerged parasitoids. Caterpillars were reared until pupation (~50 days), and pupae were housed together by site of origin (no more than ~10 per site) in 30 cm x 30 cm flight cages and allowed to emerge as moths, at room temperature. Pupae and moths were reared until one month after the last moth emerged and sprayed once or twice weekly with water to prevent desiccation. Adults do not feed. Dead pupae and moths were stored dry at room temperature for subsequent dissection. Individuals that reached adulthood fully formed were counted as having survived; individuals that died as caterpillars or failed to emerge from pupae or expand wings were counted as not surviving.

Dissection and viral assays

After death, each individual was dissected to assess infection status. Two to six tissue samples per insect were taken from the abdomen of adults and pupae or fat bodies of caterpillars, broken up with forceps, smeared on a glass slide with water, and examined under a light microscope at 200x magnification with phase contrast. Visible occlusion bodies (OB) (<0.15μm) were confirmed by adding to the slide a drop of 1 M NaOH, which dissolves the viral protein

coat, rendering the OB transparent (Lacey and Solter 2012)(Figure 4.6). Tissue samples were taken until a positive NaOH test was obtained; if no virus was found after six tissue samples, individuals were classified as uninfected (see supplemental methods for more detail).

Infection severity was rated as uninfected, low, medium, high, or very high, based on the number of samples required to discover virus, the density of OBs in tissue smear samples, and the coloration of hemolymph and fat body (Figure 4.7). Low severity infections required many samples to identify and had low densities of OBs. Medium severity infections required fewer samples to identify and had moderate densities of OBs. High severity samples had infections in all samples with high densities of OBs, with organ systems in the body still intact and identifiable. Very high severity infections had infections in all samples with very high densities of OBs, with internal organ systems unidentifiable.

Ultraviolet irradiation

Daily values for ultraviolet radiation in 2019, specifically 'Erythemal Daily Dose' in Watts/m^2 from Ozone Monitoring Instrument (OMI)/Aura satellite data were accessed from NASA GES DISC (Hovila et al. 2014). Values were extracted for each sampling location and the average value calculated from 360 to 180 days before the collection date of caterpillars (~March-September at most sites; see Table 4.2 for collection dates). This timing coincided with the season during which viral OBs would have persisted in the environment outside of hosts.

Statistical analysis

First, we analyzed the density-dependence of infection rate (proportion of infected individuals) and the influence of ultraviolet radiation on infection rate. The proportion of all individuals (N=208) that were infected was analyzed in response to log caterpillar density per m^2 from transects in 2019 (density in the previous year) and 2020 (density in the same year) using

beta-binomial generalized linear mixed models with site as a random effect. To test for the effect of ultraviolet radiation, we implemented a model with both ultraviolet radiation and log density, to control for the effect of density on infection rate.

Second, we analyzed the density-dependence of infection severity, and the influence of ultraviolet radiation on infection severity. We analyzed infection severity (N=198 with severity rated) in response to log density (same year and previous year) using cumulative link mixed models with site as a random effect. As before, to test for the effect of ultraviolet radiation, we implemented a model with both ultraviolet radiation and log density, to control for the effect of density on infection severity. To test for effects of density and ultraviolet radiation on infection severity independent of infection status, we implemented models using only infected individuals (N=184). This allowed us to test whether different processes influenced infection rate vs. infection severity. We implemented cumulative link mixed models with only log density, and both log density and ultraviolet radiation as predictors as before.

Third, we tested for density-dependent survival and effects of ultraviolet radiation on survival. We analyzed survival to emergence as fully formed moths (N=208) as a function of caterpillar density, tachinid parasitoid load, and ultraviolet radiation in a beta-binomial generalized linear mixed model with site as a random effect.

Finally, we tested our structural hypothesis that viral infection and infection severity were the mechanisms through which lagged density and ultraviolet radiation affected survival in moth populations. There are multiple possible pathways through which density, ultraviolet radiation, infection rate, and infection severity might influence survival and thus population dynamics. To test our specific structural hypothesis, we constructed a piecewise structural equation model which tested whether infection rate and infection severity mediated the effects of ultraviolet

radiation and caterpillar density on survival. To do this, we transformed infection severity into a continuous variable between 0 and 1, by converting to numerical categories from 1-5, dividing by 5, and subtracting 0.1. We constructed 3 component sub-models of our structural equation model: a beta-binomial model of infection rate predicted by log density and ultraviolet radiation, a beta model of infection severity rate predicted by infection rate, log density and ultraviolet radiation, and a beta-binomial model of survival predicted by infection rate and infection severity (Figure 4.5). All sub-models included site as a random effect, and only individuals that were not parasitized and were scored for infection severity were included in the analysis (N=198). Standardized coefficients were calculated using the latent-theoretic method (Grace et al. 2018).

Beta-binomial and beta generalized linear mixed models were fit using glmmTMB (Brooks et al. 2017). Cumulative link mixed models were fit using the ordinal package (Christensen 2019). Piecewise structural equation models were fit using piecewiseSEM v. 1.2.1 (Lefcheck 2016), and component models were fit using glmmTMB. Ultraviolet radiation was logged and scaled to improve model convergence. We checked for multicollinearity in models using VIFs; multicollinearity was low to moderate in all models (<6) except for same year density in models of infection severity (VIF from 10.5-11.5). Because we included same year density as a control variable, we kept these models as is despite high VIFs. Plots were generated using ggplot2 (Wickham 2009), ggeffects (Lüdecke 2018), and viridis (Garnier 2018). All analyses and plotting were conducted in R v. 3.6.3 (R Development Core Team 2020).

4.4 Results

Infection rate

In models of infection rate, probability of infection increased with log density in the previous year (Table 4.1, Figure 4.2a). Infection rate had little relation to log density in the current year or ultraviolet radiation (Table 4.1, Figure 4.2b).

Infection severity

In models of infection severity that included uninfected caterpillars, log density in the previous year increased infection severity, but this effect was weakened when ultraviolet radiation was included in the model (Table 4.1, Figure 4.3a,b). This may have been due to low power, or a negative correlation between log density in the previous year and ultraviolet radiation (Pearson's r: -0.53). Ultraviolet radiation decreased infection severity when included (Table 4.1, Figure 4.3c,d). In models that included only infected caterpillars, density had little effect on infection severity, and ultraviolet radiation had a negative effect on infection severity (Table 4.1).

Survival to adult emergence

In models of survival to adult emergence, survival decreased with log density in the previous year and with the number of emerged parasites, and increased in response to density in the current year, and in response to ultraviolet radiation (Table 4.1, Figure 4.4).

Structural equation model

We hypothesized a causal model linking ultraviolet radiation and disease to caterpillar survival (Fig. 4.5). Shipley's d-separation test (Shipley 2000) indicated that our structural equation model was correctly specified (Fig. 4.5, Fisher's $C = 7.38$, $df = 6$, $P = 0.288$), meaning that there were no missing paths in our causal model. The model results showed that the effect of log density in the previous year on survival was mediated by infection rate and infection severity, and that the effect of ultraviolet radiation on caterpillar survival was mediated by

infection severity (Fig 4.5). The relative indirect effect size of log density in the previous year was ~2.5x greater than the effect of ultraviolet radiation on survival (-0.085 vs 0.035, calculated by multiplying path coefficients).

4.5 Discussion

Overall, our results show that log density during the previous year increased infection rate and infection severity and decreased survival to adult emergence, suggesting a strong delayed density-dependent effect of disease on caterpillar population dynamics. The effect of delayed density on both infection rate and infection severity in univariate models and the result of the structural equation model suggest that the effect of density on survival acts through infection severity as well as infection rate. This is likely due to dose-dependent infection severity, in which caterpillars that are exposed to more viral occlusion bodies develop more severe infections that result in death (Matthews et al. 2002, Eberle et al. 2008, Cabodevilla et al. 2011).

In contrast, log density in the current year, representing direct density-dependence, had no effect on infection rate, a marginal negative effect on infection severity, and a positive effect on survival to adult emergence. Though inconsistent, this positive effect may have been due to ascertainment bias: sites that had larger viral outbreaks may have already declined in density over the course of the larval season (summer 2019-spring 2020). Therefore, density at the time of collection may have had a negative relationship with environmental OB density, the inverse of what might be expected biologically. Sites that had declined from earlier high densities would have higher levels of OB, resulting in more severe infections and a higher probability of death. Overall, our results indicated negative delayed density dependence and weak or positive direct

density-dependence consistent with the second-order, oscillatory population dynamics observed in the system over the long term (Pepi et al. 2021a).

Ultraviolet radiation by contrast had no detectable effect on infection rate but reduced infection severity and increased survival. The reduction in infection severity was even greater when only infected individuals were considered. The effect of ultraviolet radiation on infection severity and survival but not infection results may represent dose-dependent effects of exposure to OBs. Specifically, at sites with higher ultraviolet radiation, more viral OBs were likely inactivated before caterpillars could be exposed to them, so caterpillars received smaller doses of virus and thus became less severely infected and were more likely to survive.

The observational nature of our study gives it some strengths and weaknesses. Our study is one of few to show delayed-density dependent viral infection in the field, and the only study to show effects of radiation on viral infection in a natural population of insects. Our results provide validation in a field system to laboratory studies of virus dynamics and inactivation effects of ultraviolet radiation on viruses (e.g., Bjørnstad et al., 1998; Witt & Stairs, 1975). Despite highly variable conditions between sites, which were spread across a gradient of over 1000 km, we were able to detect clear effects of delayed density on infection rate, severity, and survival to adulthood, and of ultraviolet radiation on infection severity and survival to adulthood. We were also able to use structural equation modelling to show that infection rate and severity mediate the effect of delayed density and ultraviolet radiation on survival and strengthen the inferences made from our observational study.

Density in the previous year was a strong predictor of infection rates in populations (Fig 2). This finding supports the notion that there must have been a large enough population of hosts in the previous year for the disease to spread and produce sufficient inoculum to persist into the

current year. Density in the previous year also affected infection severity (Fig 3), but this effect became much weaker when ultraviolet radiation was included in models and even weaker when only infected caterpillars were considered. In the structural equation model, infection severity was well explained by infection rate because individuals must be infected to have high infection severity. This result may be due to the conflation of infection rate and infection severity in the model since the same dose-dependent mechanism may have caused them. However, in all models of infection severity that included both ultraviolet radiation and delayed density, the effect of delayed density, beyond whether individuals were infected or not, was weaker than the effects of ultraviolet radiation. Thus when effects on infection severity were detected they may have in fact been generated by the spurious negative relationship between delayed density and ultraviolet radiation. In contrast to infection severity, ultraviolet radiation had no significant effect on infection rate. Ultimately, both delayed density and ultraviolet radiation had strong and opposing effects on survival to adulthood, though the effect of density in the previous year was much greater in magnitude. The effects of delayed density on survival were mediated through infection with limited evidence of any direct effect on infection severity. In contrast the effects of ultraviolet radiation on survival were mediated entirely through effects on infection severity.

A possible explanation for the finding that infection rates are primarily determined by host density in the previous year but not by ultraviolet radiation is that viral infection may be determined in part through vertical transmission (Burden et al. 2002, Cory and Myers 2003, Cabodevilla et al. 2011, Cory 2015). In particular, vertical transmission is likely to occur in *A. virginalis* through persistent sub-lethal infections. We regularly observed OB in egg samples in adult dissections, and thus eggs of adults with sublethal infections are likely contaminated with virus. Vertical transmission represents a mechanism through which density in the previous year

might influence infection rates in the following year but is not subject to influence from ultraviolet radiation. In this way, vertical transmission may maintain higher infection rates after high-density years with epizootics, even if ultraviolet radiation attenuates inoculum in the environment (Cabodevilla et al. 2011). Sublethal infections may represent another means by which granulovirus affects population dynamics by imposing fitness costs on adults (Rothman 1997, Matthews et al. 2002, Cabodevilla et al. 2011), although we did not measure this in the present study.

In summary, we demonstrated population-level delayed density-dependent effects on viral infection rate, infection severity, and survival to the reproductive stage, showing how viral infection may drive cyclic dynamics in insects. We also showed for the first time that ultraviolet radiation may influence disease dynamics and ultimately population dynamics of insects, through decreased infection severity and increased survival rates. This provides support for the proposal that viral epizootics may be an important mechanism driving cyclic dynamics of insects and Lepidoptera in particular (Myers and Cory 2013). Our findings also suggest that ultraviolet radiation may be an important factor to consider as a driver of insect viral disease in the context of global change. In particular, long-term changes in atmospheric transmittance of solar radiation, or "global dimming and brightening," have been observed and are potentially anthropogenic in origin (Wild 2016). Such long-term changes may have the potential to influence insect viral disease and population dynamics through changing levels of ultraviolet attenuation of viral inoculum (Haynes et al. 2018).

4.6 Acknowledgements

We would like to thank Marcel Holyoak, Jenny Cory, and Jay Rosenheim for helpful comments on the manuscript. We would also like to thank California State Parks, Ben Becker at

Point Reyes National Seashore, Kristen Ward at Golden Gate National Recreation Area, Jackie Sones at Bodega Marine Reserve, Brendan Leigh at Humboldt Bay NWR, Karlee Jewell at North Coast Landtrust, Diane Steeck at the City of Eugene, Grey Wolf at the City of Salem, Oregon Metro Parks, and Christian Haaning at the City of Portland for assistance and access to field sites. We would also like to thank Harry Kaya for assistance with identifying the granulovirus, Jay Rosenheim for the use of incubators, Neal Williams for the use of compound microscopes, and Claire Beck and Jasmine Daragahi for help with rearing caterpillars. The research was funded by NSF-LTREB-1456225 and an NSF REU supplement (DEB-2018169).

4.7 Tables & Figures

Model structure	Parameter	Logit β ± 1 SE	z	P
Infection ~ log density	Log density current year	-0.20±0.38	-0.52	0.603
	Log density previous year	**0.55±0.26**	**2.10**	**0.036**
Infection ~ log density + ultraviolet	Log density current year	-0.10±0.39	0.25	0.802
	Log density previous year	**0.92±0.46**	**1.998**	**0.046**
	Ultraviolet radiation	0.66±0.58	1.13	0.259
Severity ~ log density	Log density current year	-0.28±0.19	-1.49	0.135
	Log density previous year	**0.26±0.11**	**2.35**	**0.019**
Severity ~ log density + ultraviolet	Log density current year	-0.28±0.18	-1.61	0.101
	Log density previous year	0.16±0.11	1.37	0.170
	Ultraviolet radiation	**-0.35±0.17**	**-2.04**	**0.041**
Severity | infected ~ log density	Log density current year	-0.27±0.19	-1.39	0.163
	Log density previous year	0.018±0.11	1.66	0.096
Severity | infected ~ log density + ultraviolet	Log density current year	-0.28±0.18	-1.52	0.129
	Log density previous year	0.06±0.12	0.48	0.631
	Ultraviolet radiation	**0.44±0.18**	**-2.40**	**0.017**
Survival ~ log density + ultraviolet	**Log density current year**	**1.15±0.51**	**2.25**	**0.024**
	Log density previous year	**0.75±0.31**	**-2.39**	**0.017**
	Ultraviolet radiation	**0.64±0.32**	**-1.97**	**0.049**
	Emerged parasites	**5.39±1.58**	**-3.42**	**0.0006**

Table 4.1. Results of univariate models, including logit beta parameter estimates (plus or minus one standard error), z-values, and P-values for each parameter.

Site	Latitude	Longitude	Number reared	Date Collected
Franklin Point, CA	37.155	-122.35	29	3/1/2020
Pescadero Marsh, CA	37.265	-122.41	16	3/1/2020
Golden Gate NRA, CA	37.844	-122.55	28	3/13/2020
Point Reyes South, CA	38.038	-122.99	15	3/13/2020
Point Reyes North, CA	38.088	-122.97	29	3/13/2020
Point Reyes Kehoe, CA	38.153	-122.94	2	3/13/2020
Bodega Marine Reserve, CA	38.319	-123.06	16	3/27/2020
Manchester State Park, CA	38.959	-123.72	6	3/27/2020
Loyalton, CA	39.700	-120.30	6	5/30/2020
Humboldt NWR, CA	40.670	-124.21	20	4/10/2020
Freshwater Farms, CA	40.786	-124.09	11	4/10/2020
Klamath River, Yreka, CA	41.829	-122.61	11	4/10/2020
Checkermallow Access, OR	44.072	-123.20	12	4/11/2020
Fairview Wetland, OR	44.895	-123.00	20	4/11/2020
Graham Oaks, OR	45.299	-122.80	30	4/11/2020
Powell Butte, OR	45.488	-122.50	33	4/11/2020
Salish Ponds, OR	45.531	-122.45	1	4/11/2020
West Rocky Prairie, WA	46.887	-122.87	2	4/12/2020

Table 4.2. Location, number of larvae collected and sampling date of each site.

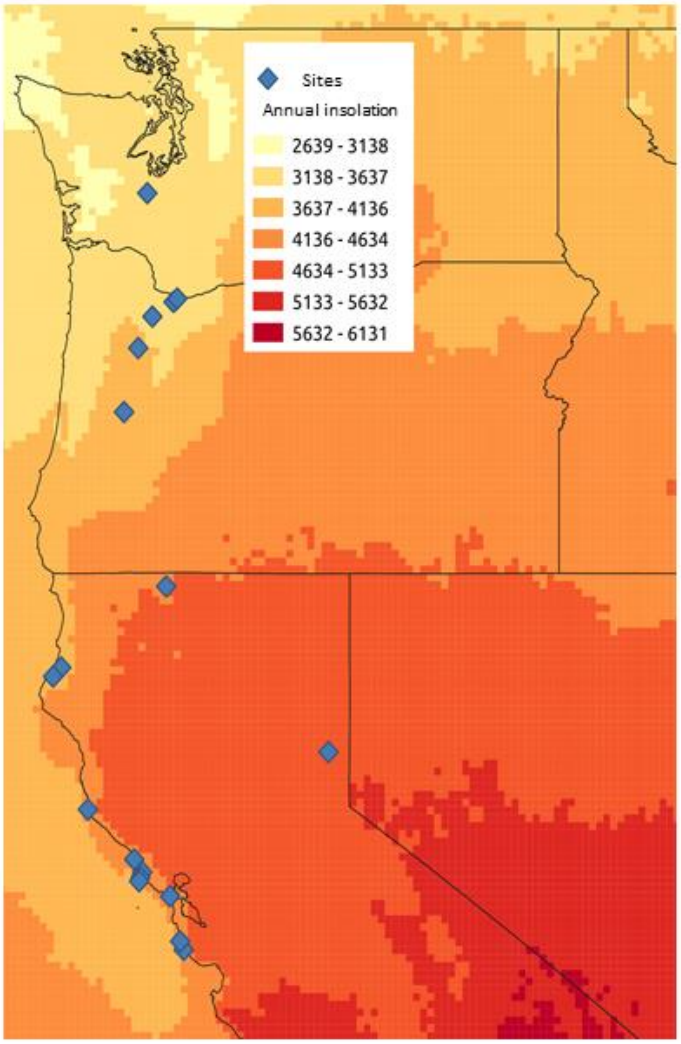

Figure 4.1. Map of study site locations in Washington, Oregon, and California, overlaid on a map of average annual solar insolation (GHI), in kWh/m^2 from 1998-2005 (NREL 2009).

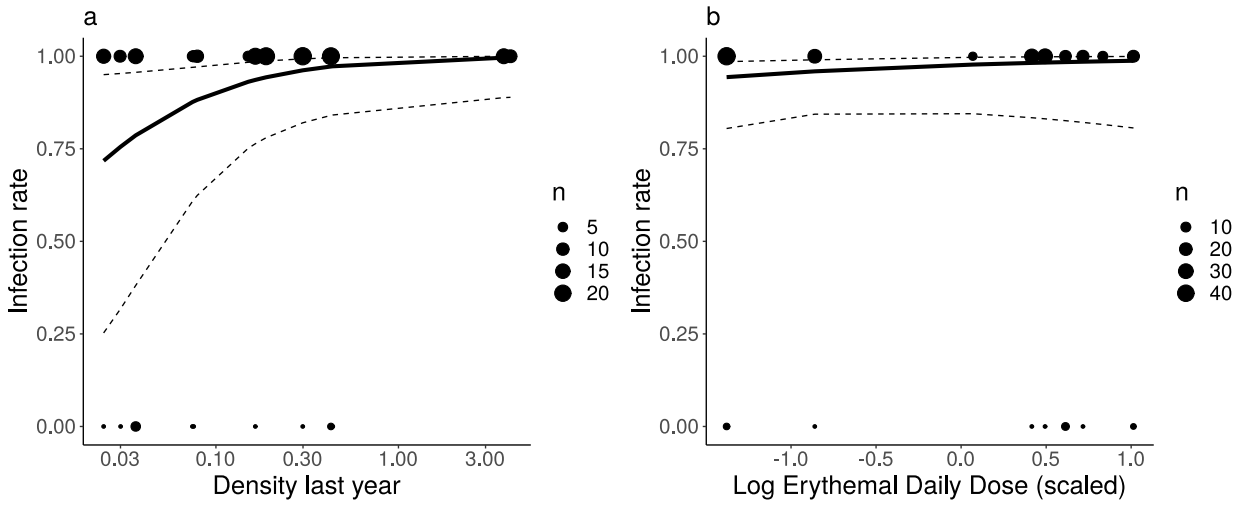

Figure 4.2. Infection rate in response to (a) density in the previous year and (b) ultraviolet radiation as scaled log erythemal daily dose in the summer before collection (2019) from beta-binomial generalized linear mixed models.

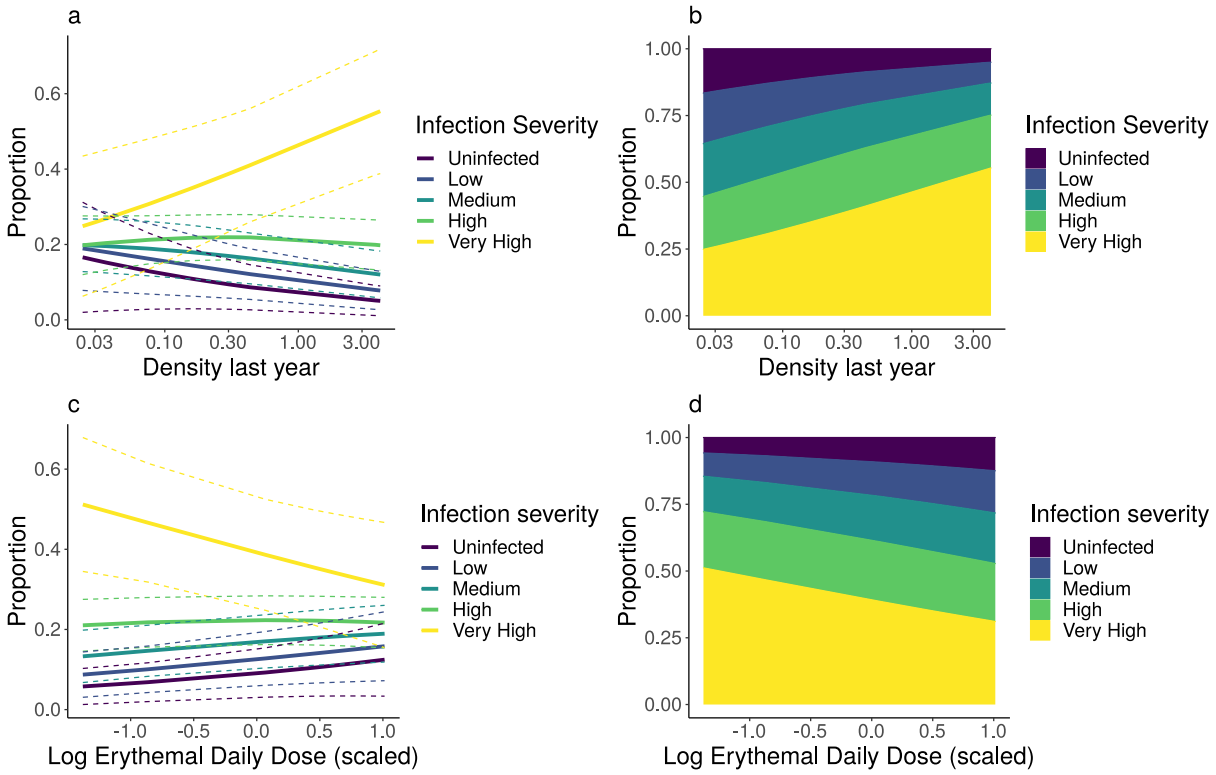

Figure 4.3. Infection severity in relation to (a-b) density in the previous year, and (c-d) ultraviolet radiation as scaled log erythemal daily dose in the summer before collection in cumulative link mixed models. The left panels (a,c) show model predicted rate of infection at each severity class with 95% confidence intervals, and the right panels (b,d) show the proportion of the total population predicted to be infected at each severity class by color.

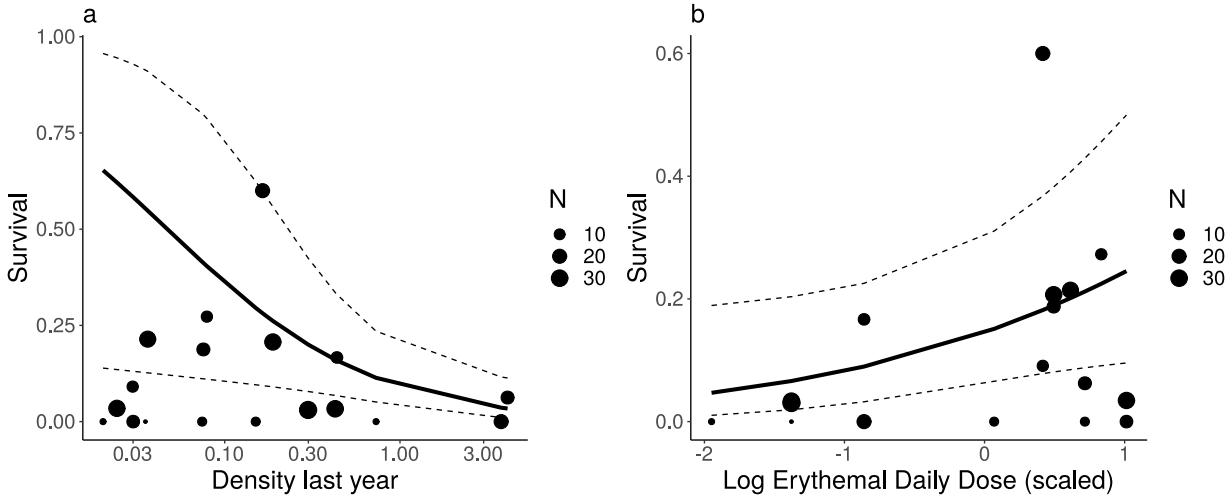

Figure 4.4. Survival to adult emergence in response to (a) density in the previous year, and (b) ultraviolet radiation as scaled log erythemal daily dose in beta-binomial generalized linear mixed models. Point size is scaled to the number of individuals reared from each site.

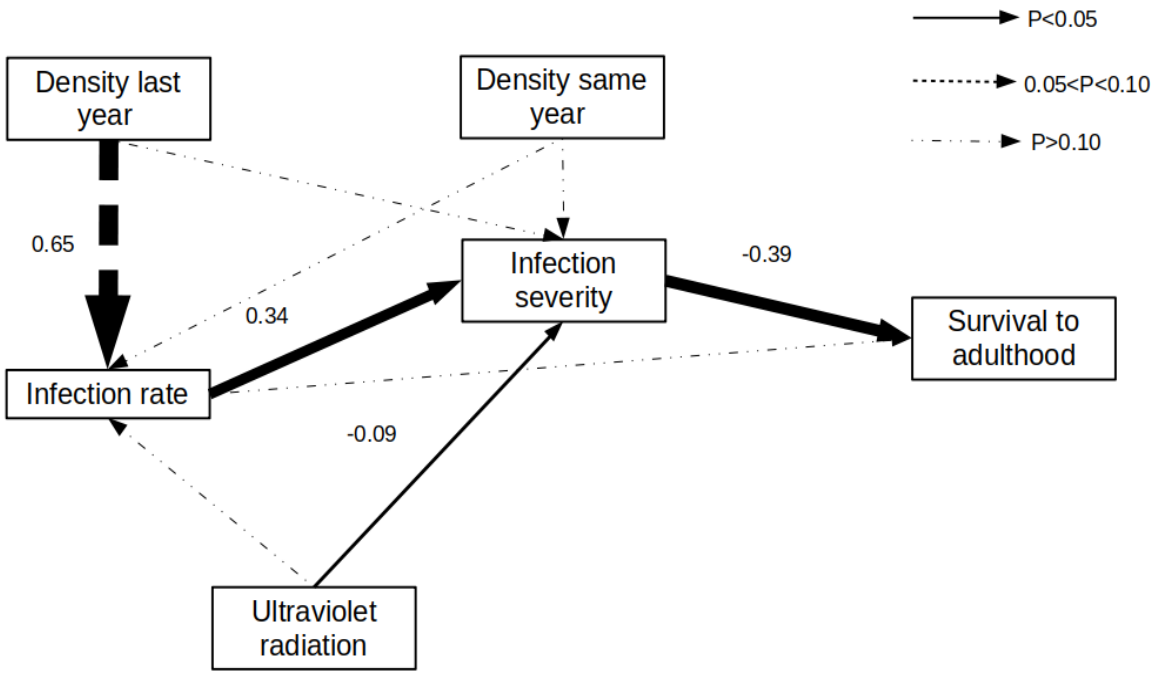

Figure 4.5. Path diagram of piecewise structural equation model of effects of density and ultraviolet radiation on survival, as meditated through baculovirus infection. Arrow size is proportional to the standardized path coefficient (shown next to lines), and line type indicates *P*-value of the path parameter.

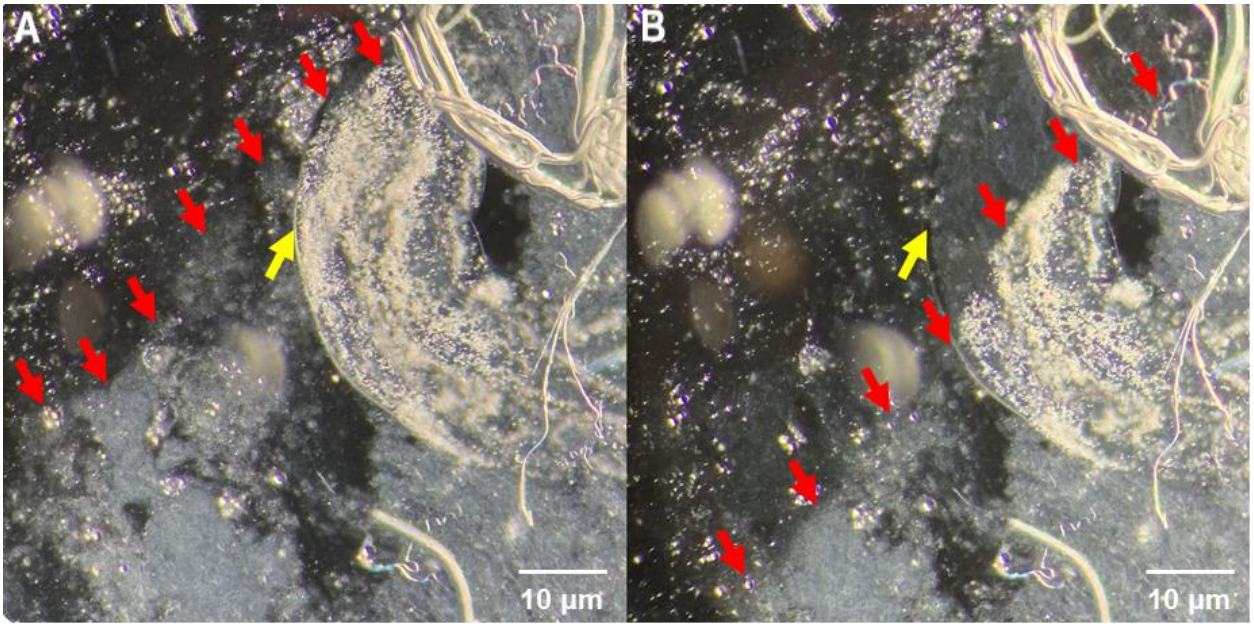

Figure 4.6. Fat body tissue smear from a caterpillar infected with GV under a light microscope at 200x magnification with phase contrast. An added drop of NaOH moved through the sample. The red arrows point to the boundary between NaOH solution and water. The yellow arrows point to the OBs (Figure A) which turned transparent (Figure B) after they were dissolved by the strong base.

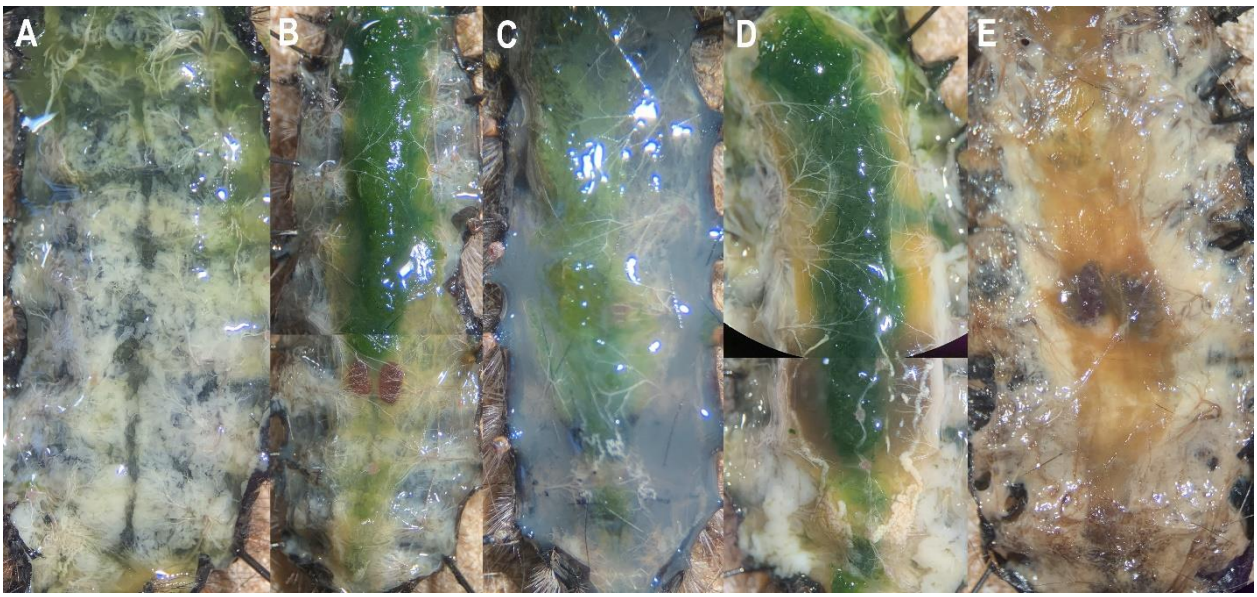

Figure 4.7. Ventral dissection of late instar *A. virginalis* larva in the order of infection severity, ranging from (A) uninfected, (B) low severity, (C) medium severity, (D) high severity, to (E) very high severity. The gut of the caterpillar in figure A is missing. Caterpillars with higher infection severity have a cloudier hemolymph and a darker and more yellowish fat body. They also often have large clusters of infected tissues next to the midgut (e.g. Figure D).

5. Chapter IV: Altered precipitation dynamics lead to a shift in herbivore dynamical regime

As published in *Ecology Letters* with Marcel Holyoak and Richard Karban (Pepi et al. 2021a)

5.1 Abstract

The interaction between endogenous dynamics and exogenous environmental variation is central to population dynamics. Although investigations into the effects of changing mean climate is widespread, changing patterns of variation in environmental forcing also affect dynamics in complex ways. Using wavelet and time-series analyses, we identify a regime shift in the dynamics of a moth species in California from shorter to longer period oscillations over a 34-year census, and contemporaneous changes in regional precipitation dynamics. Simulations support the hypothesis that shifting precipitation dynamics drove changes in moth dynamics, possibly due to stochastic resonance with delayed density-dependence. The observed shift in climate dynamics and the interaction with endogenous dynamics mean that predicting future population dynamics will require information on both climatic shifts and their interaction with endogenous density dependence, a combination that is rarely available. Consequently, models based on historical data may be unable to predict future population dynamics.

5.2 Introduction

The dynamics of populations reflect the interplay between endogenous demographic and exogenous environmental drivers. Since its inception, population ecology has focused on debates about the relative contribution of these components to the generation of several salient phenomena observed in the dynamics of natural and laboratory populations, particularly cyclic fluctuations (Nicholson 1933, Andrewartha and Birch 1954, Barraquand et al. 2017). More

recently, it has been recognized that both endogenous and exogenous drivers play important roles in generating observed population dynamics, and that endogenous deterministic dynamics and exogenous environmental noise or perturbations may combine to generate differing dynamics than would be expected for either component alone (Bjørnstad and Grenfell 2001, Turchin 2003, Barraquand et al. 2017). There has been additional motivation to understand the effects of climate on population dynamics as the effects of global climate change on the planet's biota have become more apparent (Walther et al. 2002, Parmesan 2006). Climate change is expected to result in increased climate variability (Coumou and Rahmstorf 2012), as well as alterations to patterns of large-scale climate oscillations (Simon Wang et al. 2017), both of which are important drivers of local population dynamics. In a prominent example, changes in oceanic temperature oscillation regimes have resulted in dramatic changes to precipitation patterns in California (Simon Wang et al. 2017), with large impacts to society and natural ecosystems.

Climate variation can have direct effects on interannual fluctuations in population size or may interact in complex ways with endogenous dynamics of populations. For example, environmental perturbations can sustain population oscillations that might otherwise decay to a stable equilibrium (Tomé and De Oliveira 2009, Barraquand et al. 2017). Climate change has also appeared to cause the collapse of population cycles of many species across Europe (Ims et al. 2008, Cornulier et al. 2013). Environmental perturbations with different spectra of variability can also amplify, dampen, or impose their own spectra on oscillatory populations depending on the "colour" (temporal autocorrelation) of environmental spectra relative to the spectra of the endogenous dynamics of the population (Greenman and Benton 2003). Changing climate can also interact in a non-stationary way with population dynamics, such as transient effects of long-term climate oscillations on epidemic disease cycles (Rodó et al. 2002, Cazelles et al. 2005).

However, testing for such effects on population dynamics of other kinds of organisms requires rarely available long-term population data.

In the present study, we examined how changing precipitation dynamics interact with the endogenous population dynamics of an extensively studied insect species, the Ranchman's tiger moth (*Arctia virginalis*). We analyzed 34 years of census data from northern California, over a period during which there have been significant shifts in the dynamics of regional climate (Simon Wang et al. 2017). Using time series analyses and simulations, we tested for changes in population dynamics, and compared multiple possible mechanisms for observed shifts. Using simulations, we tested the hypotheses that shifting dynamics were because 1. underlying dynamics were first masked and later amplified by precipitation, 2. underlying dynamics were first amplified and later masked by precipitation, or 3. dynamical shifts were driven completely exogenously by changing precipitation dynamics.

5.3 Materials and Methods

Description of system

Ranchman's tiger moth (*Arctia virginalis*) is a univoltine, day-active Arctiine moth, native to much of the western United States. Adult moths emerge in late spring or early summer and have a flight period of several weeks during which they do not feed. Eggs are laid on low vegetation or litter in early summer; small caterpillars hatch soon after eggs are laid. Early instar caterpillars are heavily preyed upon by ground nesting ants, and are potentially food-limited during seasonal senescence of vegetation in Mediterranean summers (Karban et al. 2013, 2017). Time series analyses have shown that greater precipitation during the previous year results in greater population growth, possibly due to increased food availability during the summer drought (Karban and de Valpine 2010, Karban et al. 2017). Caterpillars feed continuously over the winter

period and do not diapause in California. After this, they move up to feed on higher vegetation and become more visible in late winter in California. Caterpillars are generalists, with a preference for alkaloid-containing hosts (English-Loeb et al. 1993, Karban et al. 2010). Caterpillars are also frequently attacked by tachinid parasitoids, *Thelaira americana* (Karban and de Valpine 2010), which are specialists on Arctiine moths (Arnaud 1978), and may functionally be specialists on Ranchman's tiger moth at our study site, the Bodega Marine Reserve. However, analyses have suggested that parasitism has little effect on caterpillar population dynamics (Karban and de Valpine 2010). Caterpillar populations at the Bodega Marine Reserve and other sites often exhibit high mortality rates after high population density years due to a granulovirus. Monitoring at Bodega and other sites has shown delayed density-dependent infection and mortality rates due to granulovirus (Pepi et al. 2021b).

Censuses

Caterpillar censuses were conducted on perennial evergreen yellow bush lupine (*Lupinus arboreus*) bushes at Bodega Marine Reserve in Sonoma County, California (38°19'05"N, 123°04'12"W). The number of caterpillars on 10 lupine bushes in the same patch were counted yearly from 1986 to 2019 (>10 in 1986). Bushes were censused in the last week of March each year. Previous repeated censuses within a year between late February and the end of March suggest that population estimates were unlikely to vary significantly due to changes in seasonal phenology from year to year (Karban and Grof-Tisza, unpublished data), because of the long development period of caterpillars and their limited mobility during this stage. The same lupine bushes were censused each year; however, the identity of bushes changed because these lupines were short lived (< 7yr). To account for variation in sampling effort, area of each lupine bush censused was measured to calculate caterpillar density per m^2 (plotted as caterpillars per 100 m^2

in Figure 5.1 for legibility). Precipitation was recorded at the site as part of ongoing climate monitoring by the University of California and using a rain gauge at the study site (US Weather Bureau type manual rain gauge prior to 1992 and an optical rain gauge ORG-815, Optical Scientific, Gaithersburg, MD since 1992 with a Hydrological Services TB4 tipping bucket, Campbell Scientific, Ogden, UT since 2003). For analyses, total annual precipitation within the hydrologic year was calculated (from October 1st of the previous year to September 30th of the current year).

Statistical analyses

To test for non-stationary relationships between precipitation and caterpillar dynamics over time, wavelet analysis was conducted separately on logged and scaled caterpillar and scaled precipitation time series, and as wavelet coherence analyses on both series (Figure 5.1). Scaling was accomplished by subtracting the mean and dividing by the standard deviation (scale() in R). Analyses were conducted using the package BIWAVELET (Gouhier et al. 2019), using Morlet wavelet transforms. In addition, change-point analyses were conducted using the SEGLM and TSDYN packages (Antonio and Stigler 2009, Stigler 2019), with a model containing direct and delayed density-dependence, and a separate model also including precipitation as a covariate. We included precipitation as a covariate based on previous knowledge that precipitation was important to dynamics. We included direct density-dependence based on previous detection in time series analyses (Karban and de Valpine 2010), and delayed density-dependence based on wavelet periodogram results and the observation of delayed-density dependent mortality from granulovirus in field studies (Pepi et al. 2021b). Models with and without a threshold (*C*) were compared using AIC. Break point models were of the form:

$$X_t \sim Normal(\ a_{0,1} + a_{1,1}X_{t-1} + a_{2,1}X_{t-2} + \beta_{1,1}Precip_{t-1}, \sigma_1^2)\ \ |\ \ t \leq C$$

$$X_t \sim Normal\left(a_{0,2} + a_{1,2}X_{t-1} + a_{2,2}X_{t-2} + \beta_{1,2}Precip_{t-1}, \sigma_2^2\right) \mid t \geq C,$$

in which X_t is log population density [$ln(count/area)$], a_0 is the intercept, a_1 is direct density dependence, a_2 is delayed density dependence, and β_1 is the effect of precipitation, σ^2 is the variance, with a separate parameter estimate for each before and after the threshold.

Bayesian state space population models using a Poisson observation process were constructed to test for direct and delayed density-dependence and effects of precipitation. We conducted this as a separate step from testing for thresholds to avoid identifiability issues due to limited data availability. We primarily examined a model with the same process structure as breakpoint models, including direct and delayed density dependence and an effect of precipitation, based on *a priori* knowledge about the system. For comparison, models with all possible combinations of variables were generated and compared using WAIC (Vehtari et al. 2017). State space models were fit to the time series from 1986-2004 and 2004-2019 separately and results compared, based on findings of change-point analyses. The full state-space model was of the form:

$$Y_t \sim Poisson(\exp(X_t) * area_t)$$

$$X_t \sim Normal(a_0 + a_1X_{t-1} + a_2X_{t-2} + \beta_1Precip_{t-1}, \sigma^2),$$

in which Y_t is caterpillar count, X_t is the estimated population density state on a log scale, $area_t$ is the area of lupine sampled, a_0 is the intercept, a_1 is direct density dependence, a_2 is delayed density dependence, β_1 is the effect of precipitation, and σ^2 is the process variance. Models were fitted in JAGS with interface in R using RJAGS (Plummer 2019) and R2JAGS (Yu-Sung Su and Yajima 2015). We used a vague regularizing Gaussian prior for all parameters [$Normal(0, 10)$], except for the process variance (σ^2), for which we used a uniform prior [$Uniform(0, 10)$]. Model convergence was assessed using the CODA (Martyn et al. 2019)

package, by visualizing chains and the $\hat{R}$ convergence criterion (Gelman and Rubin 1992). We also conducted one-step ahead simulations as posterior predictive checks, for which P-values were 0.5±0.03, indicating acceptable model fit. Models were fitted using 3 MCMC chains of 20,000 iterations, with 1,000 iterations of burn-in. All $\hat{R}$ values were <1.001.

To ascertain the mechanisms driving shifts in dynamics, we conducted deterministic simulations by projecting populations into the future using parameter values sampled from the posteriors of fitted state space process models. Simulations were also conducted with fitted density-dependence parameters, but with all precipitation effects drawn from the posterior of the model with the highest estimated effect of precipitation (from the second half of the series; β_1=0.922). Another simulation was conducted using the fitted process model from the second part of the series, but with density-dependent parameters (a_1, a_2) set to zero. For simulations, observed starting population sizes were used, and observed precipitation values were used for the entire period. For each mechanistic scenario, 10,000 simulations were conducted, each based on a separate draw from posteriors. Simulated population trajectories were wavelet transformed, and a dissimilarity relative to the true population series was calculated based on the method of Rouyer *et al.* (2008b) (Table 5.3), all using BIWAVELET (Gouhier et al. 2019).

5.4 Results

Caterpillar population dynamics exhibited a clear regime shift during our study. Wavelet spectrograms show that dominant oscillatory periods of caterpillar and precipitation dynamics shifted from short-period (2-3 yr) to long-period oscillations (4-6 yr; Figure 5.1c,e), though periodicity was only significant at the 95% level for precipitation in the first part of the series (2-3 yr periodicity from ~1992-1999) and caterpillars in the second part of the series (4-6 yr

periodicity from ~2003-2013). Precipitation dynamics changed after ca. 1999, and caterpillar dynamics changed shortly thereafter (ca. 2002). Wavelet coherence between precipitation and caterpillar numbers shifted from a 3-year period in the early part of the series to a 3-6 year period after ca. 2005 (Figure 5.1g), suggesting a role of precipitation in shifts in caterpillar population dynamics. The observed shift in precipitation dynamics in turn was likely caused by shifting oceanic climate oscillations; the Pacific Decadal Oscillation and offshore sea surface temperature switched from a warm to a cold phase after 1999, which resulted in shifts in dynamics of several marine species at that time (Cloern et al. 2010, Thomson et al. 2010). A similar climate regime of high-amplitude, long-period oscillations between multi-year drought and high precipitation is expected to be the norm for California in the future (Swain et al. 2018).

Change-point analyses found a change in dynamics with a threshold in 2002 (ΔAIC=4.8 relative to model without a threshold) in a model without precipitation, or in 2004 in a model including precipitation (ΔAIC=6.5). Before the threshold, direct density-dependence was estimated to be negative and this became positive after the threshold, though there was limited evidence that these estimates were different from zero ($0.10>P>0.09$; see Table 5.1). In models that included precipitation, its effects were always near zero before the threshold, and strongly positive after the threshold (Table 5.1). Delayed density-dependence had negative parameter estimates in all models, with the most evidence for delayed density dependence after the threshold in the model without precipitation ($P=0.019$), and weaker evidence otherwise ($P>0.2$).

Results from Bayesian Poisson state-space models corresponded broadly with those from the change point analyses, showing a shift in dynamics from the first to the second period. The full model was an acceptable fit relative to other model structures tested, though large differences were not detected due to the state-space structure and limited data availability (Table

5.2; ΔWAIC<2 for all models). 90% high density posterior intervals (HDPI) that are superior for characterizing MCMC posteriors (because of more samples in the tails; Kruschke 2014) show the following: Considering the full model fitted to the entire series (1986-2019), direct density-dependence was weak (a_1 =-0.11; 90% HDPI: -0.23 – 0.47), delayed density-dependence was negative (a_2 =-0.3 ; 90% HDPI: -0.63 – 0.03]), and there was a weak positive effect of rainfall (β_1 =0.30; 90% HDPI: -0.08 – 0.70; Figure 5.2). For the first part of the series (1986-2004), direct density-dependence was negative (a_1 =-0.63; 90% HDPI: -1.19 – -0.10), delayed density-dependence was negative but weak (a_2 =-0.27; 90% HDPI: -0.78 – 0.26), and the effect of precipitation was weak (β_1 =0.26; 90% HDPI: -0.17 – 0.68; Figure 5.2). For the second part of the series (2004-2019), direct density-dependence was positive (a_1 =0.46; 90% HDPI: 0.03 – 0.82), delayed density-dependence was negative but weak (a_2 =-0.19; 90% HDPI: -0.63 – 0.36), and the effect of precipitation was stronger and positive (β_1 =0.92; 90% HDPI: 0.2 – 1.75; Figure 5.2). Overall, the results of these models provide evidence for a shift from negative to positive direct density-dependence from the first to the second part of the series, with non-overlapping 90% intervals between the two parts (a_1 =-1.19 – -0.13 vs. 0.03 – 0.82), although 95% intervals did have a marginal overlap (a_1 =-1.29 – 0.03 vs. -0.05 – 0.96; Figure 5.2). This corresponds with a shift from type III to type IV dynamics (Figure 5.3) and a shift from shorter to longer period dynamics.

The results from simulation analyses suggested that the long-period dynamics observed in the second part of the series (2004-2019) could best recreate the observed dynamics. Specifically, there was some evidence that endogenous dynamics as parameterized from the second part of the series best recovered the observed shift in dynamical regime when used to simulate dynamics for the entire series, based on the maximum *a posteriori* dissimilarity

calculated from wavelet transforms (Figure 5.4,Table 5.3; Rouyer *et al.* 2008; Gouhier *et al.* 2019). This was the case both in simulations which used the original fitted precipitation parameters, and in simulations in which the effect of precipitation was set to the same value to examine solely the effect of different endogenous dynamics (lowest dissimilarity: d=17.6; whole series: d=22.1, 18.5; first part: d=22.8, 21.4; Figure 5.4, Table 5.3). Simulations including density-dependence reproduced dynamics somewhat better (d=17.6) than simulations without density-dependence (d=19.7). The broad posterior intervals of simulation results indicated substantial uncertainty as to the mechanisms driving observed shifts (Figure 5.4). However, to the extent that we are interested in the question of whether specific endogenous dynamics (i.e., specific parameter values) underlie the observed shift in dynamics, the point estimates from the second part of the series best reproduced dynamics. Overall, results were consistent with the interpretation that the shift in dynamics was driven either by an interaction between endogenous dynamics and precipitation, or possibly solely by precipitation (Figure 5.4).

5.5 Discussion

Our analyses together suggest that over the census period, the changing structure of variation in precipitation dynamics interacted with the structure of endogenous dynamics of caterpillar populations to generate novel dynamics. This resulted in higher amplitude, long-period oscillations in the second part of the series (2004-2019), in which both the lowest (2005) and the highest (2019) caterpillar population densities were observed. This is in contrast with the first part of the census (1986-2004) which was characterized by weak lower amplitude and short-period oscillations. These shifts in oscillatory period corresponded with a shift from negative direct and delayed density-dependence (type III dynamics) to positive direct and negative delayed density dependence (type IV dynamics). Although many parameter posterior intervals

overlapped zero, there was strong statistical evidence for our main hypothesis, showing a shift from negative to positive direct density-dependence during the study (Figure 5.2,5.3). This shift in dynamics appears to have been due to changing patterns of variation in environmental forcing and illustrates the complexity of forecasting impacts of changes in both mean and pattern of variation in future climates on population dynamics.

Simulation studies have shown that environmental noise can resonate with the dominant period of deterministic endogenous dynamics of a system if the noise spectra includes the period of the deterministic system (Royama 1992, Alonso et al. 2007). Environmental variation may also impose its own spectral signature on population dynamics with different dominant periods (Greenman and Benton 2003). Given these observations, there are multiple possible mechanistic explanations for the shift in dynamics observed in this study. One possible interpretation is that the interaction between the endogenous dynamical structure of this population with changing exogenous perturbation (i.e., precipitation) obscured the endogenous dynamics in one part of the series, but not the other (Ranta et al. 2000). Another interpretation is that dynamical shifts may have been entirely externally forced by changing precipitation dynamics. We distinguished between these possibilities by simulating deterministic population trajectories from fitted state-space models using observed precipitation, which indicated that the dynamics from the second part of the series were somewhat more likely to have represented the underlying endogenous dynamics of the system. This indicates that short-period oscillations in precipitation may have interfered with delayed density-dependence in the endogenous dynamics to generate the observed population dynamics in the first half of the caterpillar time series. By imposing short-period oscillations onto population dynamics, external forcing by precipitation may have created only the appearance of negative direct density-dependence. During the second half of the series,

longer period oscillations of precipitation may have resonated with delayed density-dependence and generated high-amplitude long-period oscillations. This interpretation is supported by the fact that simulations including negative direct density-dependence (*i.e.*, the model from the first part of the series) prevented the resonance of precipitation with delayed density-dependence and did not recreate the original dynamics quite as effectively as models with positive direct density-dependence (Figure 5.4, Table 5.3). Furthermore, the possibility that observed shifts in dynamics were driven completely externally by precipitation seems less likely because simulations lacking density-dependence did not as effectively recover the original shift in dynamics as simulations including density-dependence. However, if we consider the uncertainty of parameter estimates in the simulation results, we cannot be confident in distinguishing between alternative scenarios, as all simulation posteriors overlap substantially (Figure 5.4). Nonetheless, despite the limited information contained within our 34-year population time series, our simulations allowed us to compare the relative evidence for alternate mechanisms that might have caused the observed shift.

The dynamics that we describe during the first part of the series are consistent with previous work, which indicated that precipitation positively affects caterpillar population growth rates and interacts with endogenous dynamics of overcompensating negative direct density-dependence (Karban and de Valpine 2010, Karban et al. 2017). Mechanisms proposed to explain the effect of precipitation include limited resources during summer drought (Karban and de Valpine 2010), or negative effects of precipitation on predatory ants (Karban et al. 2017). Parasitism and viral infection are potential mechanisms for both direct and delayed density-dependence in this population, as they are in many insects and particularly Lepidoptera (Myers and Cory 2013, 2016). Parasitism and viral infection can induce density-dependence in insect

population dynamics when parasitoids are host-specific and display numerical responses to host density, and when virus transmission depends on host density (Myers and Cory 2013). Delays in the action of density-dependence may be caused by delayed numerical responses of parasitoids (Myers and Cory 2013), or a greater prevalence of covert viral infections or viral occlusion bodies in the environment after high-density years (Myers and Cory 2016). Long-term monitoring data revealed no delayed density-dependent parasitism in this population (Karban and de Valpine 2010). However, laboratory rearing of *A. virginalis* from multiple monitored populations suggested a delayed-density dependent rate of viral infection (Pepi et al. 2021b) as is the case in many Lepidoptera (Anderson and May 1980, Myers and Cory 2013, 2016).

In contrast, the dynamics of the second part of the series (2004-2019) were not predictable from our previous understanding of caterpillar population dynamics derived from analyses of time series that were long by ecological standards (20 years, 1986-2006; Karban & de Valpine 2010). This type of non-stationarity due to shifts in climatic regimes has large implications for forecasting and managing populations of threatened or pest species, because such shifts have the potential to obfuscate predictions about management actions. Ecological forecasting has become an urgent goal in light of global change and unprecedented human pressures on the biosphere (Clark et al. 2001). Whereas most literature has focused on predicting ecological state variables (e.g., population size; Dietze 2017) , we examined how changing patterns of climate interacted with endogenous population drivers to qualitatively change dynamics. This illustrates the importance of considering the interaction between endogenous population drivers and exogenous climate variation in projecting population dynamics into the future, and argues that incorporating changes in patterns of climate into predictions is essential.

The fact that the qualitative range of dynamics in populations is to some extent limited (i.e., there are not ten million types of population dynamics; Lawton 1992) makes predicting shifts in population dynamics due to climate change a more attainable prospect. Consistent with this, most populations have either first or second order, and either chaotic or non-chaotic dynamics (Types I-IV and I'-IV' in Fig. 2; also see Royama 1992), in addition to some other important axes of variation (Turchin 2003, Barraquand et al. 2017). Ecologically, the presence of overcompensating (type II-III) density dependence, a stable equilibrium (type I), or longer period cycles (type IV) have important effects on species interactions, ecosystem dynamics, and how climate is likely to affect dynamics (Ranta et al. 2000, Ims et al. 2008). Mechanistic studies separating endogenous from exogenous components of dynamics can distinguish whether observed dynamics, such as cycles, arise from different mechanisms. Some of these mechanisms include self-sustaining or noise-sustained second order dynamics, externally-forced first order dynamics (Barraquand et al. 2017), and non-cyclic dynamics that mask endogenous second-order dynamics, as we found support for in the present study (Greenman and Benton 2003). The application of methods such as those implemented in the present study can help distinguish between different possible combinations of endogenous and exogenous components of a system that might have generated the observed dynamics. Doing so will improve our ability to understand how changes in exogenous forcing due to climate change are likely to affect future population dynamics.

5.6 Acknowledgments: Many former students of RK contributed to census data collection, and this work would not have been possible without them. These censuses were conducted at the UC Bodega Marine Reserve and we thank Peter Connors and Jackie Sones for facilitating our work there. We would also like to thank Eric Post, Jay Rosenheim, Rolf Ims, and Louis Botsford

for help improving the manuscript. This work has been supported by NSF, most recently NSF-LTREB-1456225

5.7 Tables & Figures

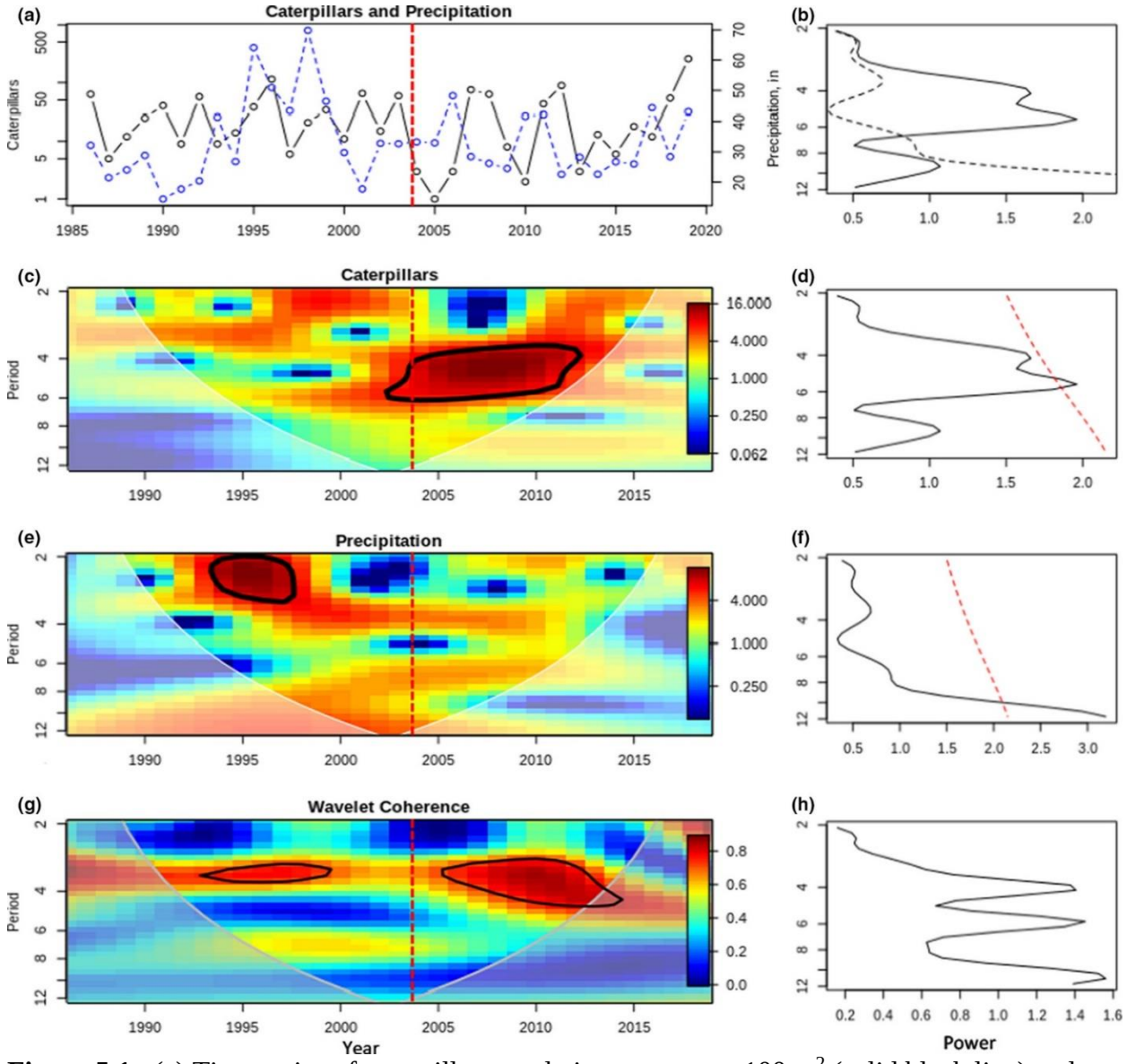

Figure 5.1: (a) Time series of caterpillar population counts per 100 m^2 (solid black line) and total annual precipitation (dashed blue line); (c) local wavelet transform of caterpillar population counts; (e) local wavelet transform of total annual precipitation; (g) wavelet coherence between total annual precipitation and caterpillar population counts; (b,d,f) global spectra of (a,c,e); (h) global coherence of (g), total annual precipitation and caterpillar population counts. The dashed red line through (a,c,e,g) represents the time threshold found in the change-point analysis including precipitation. Caterpillar density and spectral period are shown on a log scale; total

annual precipitation is shown on the right axis. Solid black lines in (c,e,g) delimit regions of significant periodicity or coherence at a 95% confidence level from a bootstrap test. Color bars in (c,e,g) show the scale power from low (blue) to high (red). Caterpillar wavelet spectrum is shown in (a) with a solid line, and precipitation wavelet spectrum is shown with a dashed line. Dashed red lines in (d,f) show the 95% confidence threshold from a bootstrap test; peaks to the right of the line represent significant periodicity.

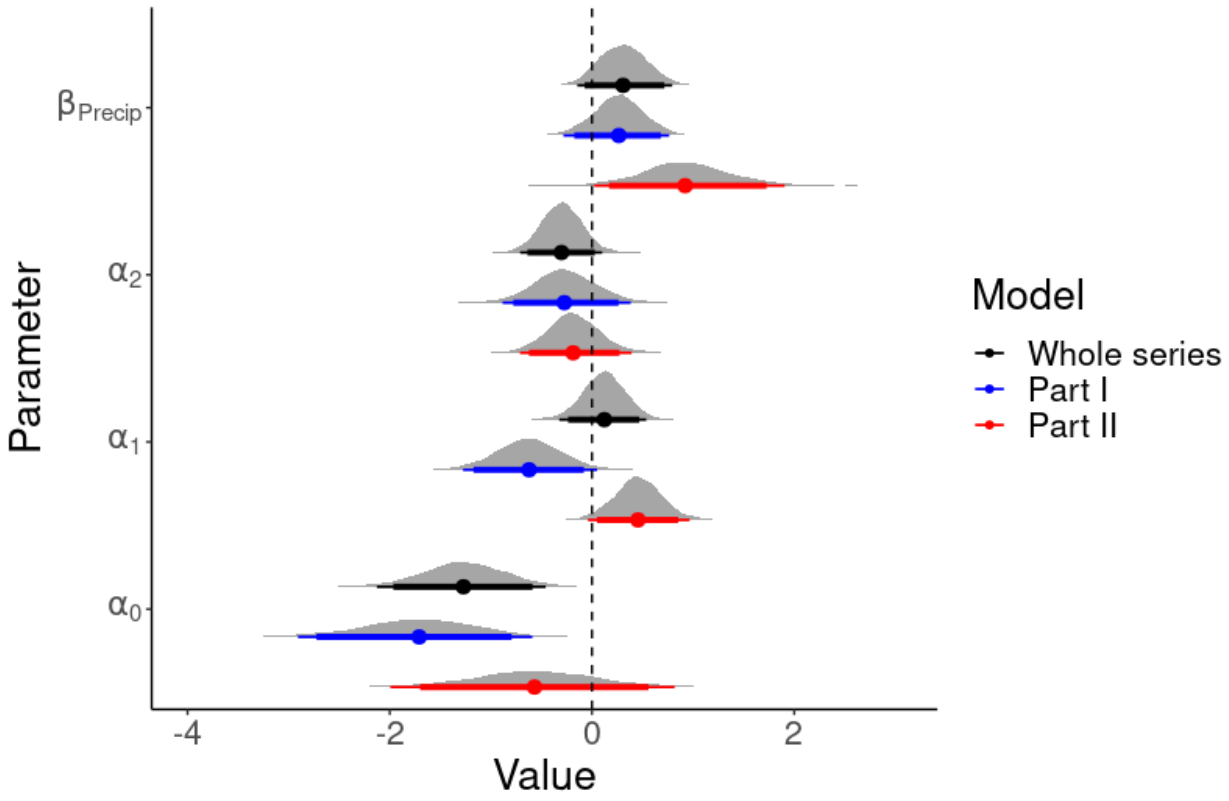

Figure 5.2: Bayesian posterior 90% and 95% (broad to narrow lines) posterior intervals, and point estimates of parameters from Poisson state-space models. Estimates from the whole series are shown in black (1986-2019), before the threshold in blue (1986-2004), and after the threshold in red (2004-2019).

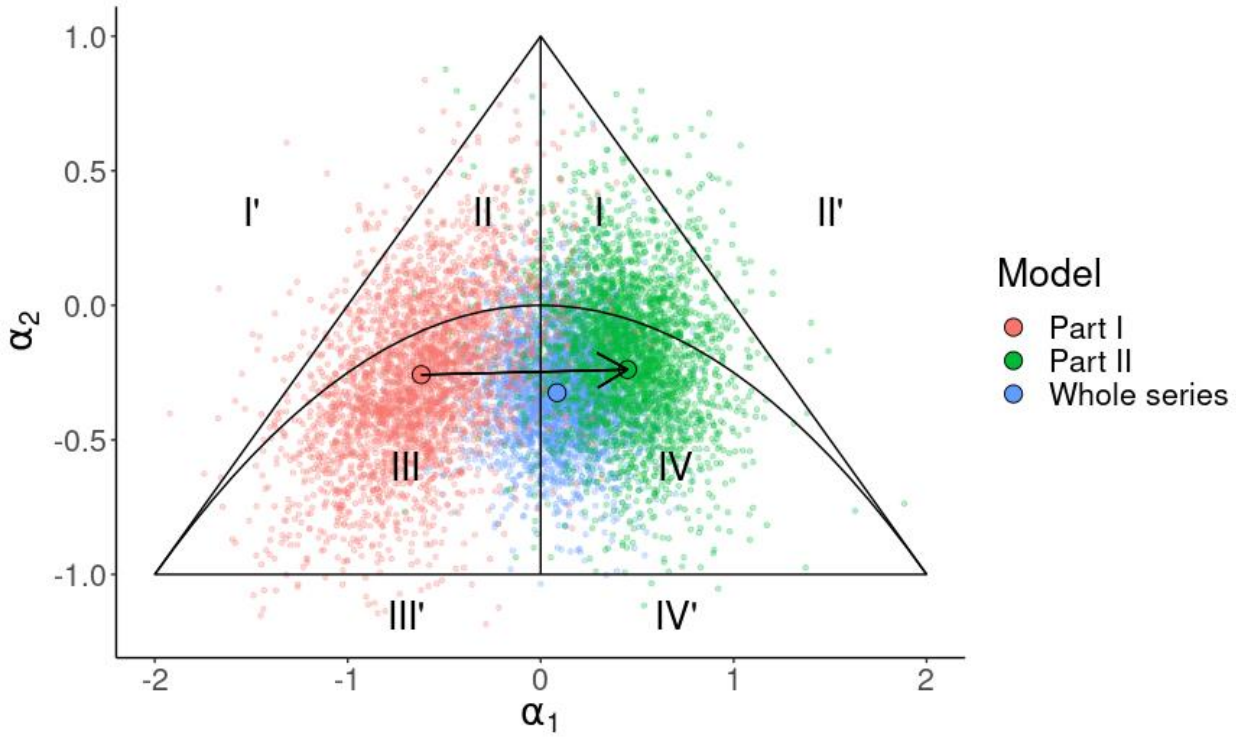

Figure 5.3. Posterior distributions of Bayesian state space models fit to the first part of the series (1986-2004), the second part of the series (2004-2019) and the whole series (1986-2019), plotted in the Royama parameter plane, showing a shift from type III to type IV dynamics. Open circles represent the median of the posterior distributions.

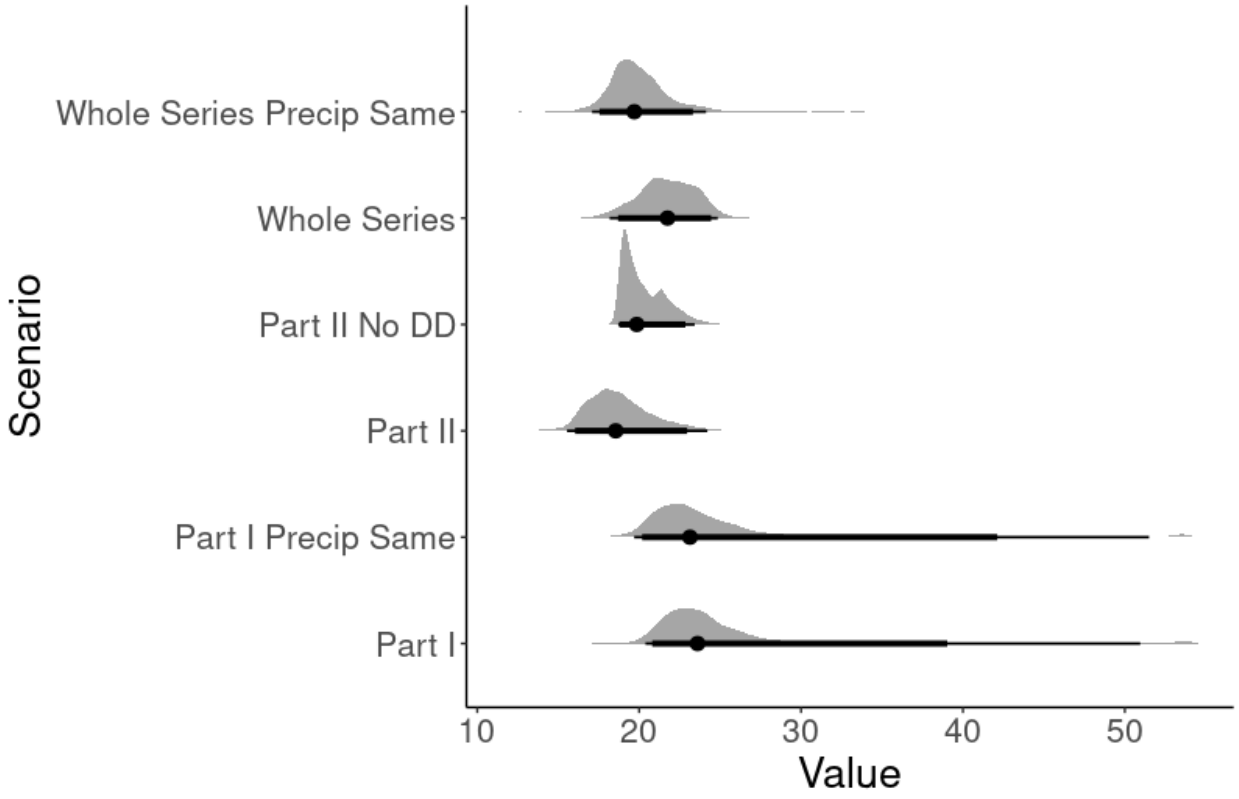

Figure 5.4. Simulation 90% and 95% (broad to narrow lines) posterior intervals and point estimates of dissimilarity values relative to the true population trajectories, from multiple mechanistic scenarios.

Model	Period	$a_{1\,[P]}$	$a_{2\,[P]}$	$\beta_{1[P]}$
Without Precipitation	**1986-2002**	-0.56 [P=0.098]	-0.44 [P=0.211]	
	2002-2019	0.35 [P=0.109]	-0.52 [P=0.019]	
With Precipitation	**1986-2004**	-0.57 [P=0.091]	-0.41 [P=0.209]	-0.01 [P=0.098]
	2004-2019	0.510 [P=0.027]	-0.286 [P=0.218]	1.27 [P=0.026]

Table 5.1. Results of change-point analysis, including parameter estimates and P values, from models with and without precipitation, before and after change-point thresholds.

Process model	ΔWAIC	WAIC	a_0 [2.5%,97.5%]	a_1 [2.5%,97.5%]
1986-2019:				
$X_t \sim a_0 + a_1 X_{t-1} + a_2 X_{t-2} + \beta_1 Precip_{t-1}$	1.38	201.78	-1.28 [-2.13, -0.46]	0.11 [-0.31, 0.53]
$X_t \sim a_0 + a_1 X_{t-1} + \beta_1 Precip_{t-1}$	1.00	201.40	-1.01 [-1.50, -0.52]	0.03 [-0.29, 0.35]
$X_t \sim a_0 + a_1 X_{t-1} + a_2 X_{t-2}$	1.36	201.76	-1.34 [-1.62, -0.52]	0.11 [-0.32, 0.53]
$X_t \sim a_0 + a_1 X_{t-1}$	0.96	200.76	-1.05 [-1.75, -0.36]	0.05 [-0.37, 0.46]
$X_t \sim a_0 + \beta_1 Precip_{t-1}$	**0.0***	**200.4***	0.05 [-0.28, 0.38]	-
$X_t \sim a_0$	0.13	200.53	0.04 [-0.59, 0.68]	-
1986-2004:				
$X_t \sim a_0 + a_1 X_{t-1} + a_2 X_{t-2} + \beta_1 Precip_{t-1}$	0.52	117.37	-1.74 [-2.92, -0.61]	-0.63 [-1.29, 0.03]
$X_t \sim a_0 + a_1 X_{t-1} + \beta_1 Precip_{t-1}$	0.57	117.41	-1.48 [-2.17, -0.81]	-0.57 [-1.10, -0.03]
$X_t \sim a_0 + a_1 X_{t-1} + a_2 X_{t-2}$	**0.00***	**116.85***	-1.68 [-2.87, -0.55]	-0.57 [-1.23, 0.08]
$X_t \sim a_0 + a_1 X_{t-1}$	0.11	116.96	-1.46 [-2.17, -0.78]	-0.53 [-1.06, -0.03]
$X_t \sim a_0 + \beta_1 Precip_{t-1}$	0.72	117.57	-0.17 [-1.06, 0.72]	-
$X_t \sim a_0$	0.81	117.66	-0.18 [-1.03, 0.68]	-
2004-2019:				
$X_t \sim a_0 + a_1 X_{t-1} + a_2 X_{t-2} + \beta_1 Precip_{t-1}$	**0.00***	**86.32***	-0.58 [-1.98, 0.79]	0.46 [-0.05, 0.96]
$X_t \sim a_0 + a_1 X_{t-1} + \beta_1 Precip_{t-1}$	1.65	87.97	-0.22 [-1.50, 0.96]	0.60 [0.01, 1.15]
$X_t \sim a_0 + a_1 X_{t-1} + a_2 X_{t-2}$	0.53	86.85	-1.30 [-2.78, 0.06]	0.340 [-0.23, 0.89]
$X_t \sim a_0 + a_1 X_{t-1}$	1.13	87.45	-0.72 [-2.27, 0.71]	0.35 [-0.32, 1.00]
$X_t \sim a_0 + \beta_1 Precip_{t-1}$	1.76	88.08	0.45 [-0.35, 1.23]	-
$X_t \sim a_0$	1.02	87.34	0.33 [-0.79, 1.46]	-

Process model	a_2 [2.5%,97.5%]	β_1 [2.5%,97.5%]
1986-2019:		
$X_t \sim a_0 + a_1 X_{t-1} + a_2 X_{t-2} + \beta_1 Precip_{t-1}$	-0.30 [-0.70, 0.01]	0.30 [-0.18, 0.78]
$X_t \sim a_0 + a_1 X_{t-1} + \beta_1 Precip_{t-1}$	-	0.36 [0.01, 0.70]
$X_t \sim a_0 + a_1 X_{t-1} + a_2 X_{t-2}$	-0.35 [-0.750, 0.05]	-
$X_t \sim a_0 + a_1 X_{t-1}$	-	-
$X_t \sim a_0 + \beta_1 Precip_{t-1}$	-	0.40 [0.018, 1.04]
$X_t \sim a_0$	-	-
1986-2004:		
$X_t \sim a_0 + a_1 X_{t-1} + a_2 X_{t-2} + \beta_1 Precip_{t-1}$	-0.27 [-0.89, 0.34]	0.26 [-0.27, 0.78]
$X_t \sim a_0 + a_1 X_{t-1} + \beta_1 Precip_{t-1}$	-	0.27 [-0.24, 0.77]
$X_t \sim a_0 + a_1 X_{t-1} + a_2 X_{t-2}$	-0.26 [-0.90, 0.38]	-
$X_t \sim a_0 + a_1 X_{t-1}$	-	-
$X_t \sim a_0 + \beta_1 Precip_{t-1}$	-	0.09 [-0.81, 0.98]
$X_t \sim a_0$	-	-
2004-2019:		
$X_t \sim a_0 + a_1 X_{t-1} + a_2 X_{t-2} + \beta_1 Precip_{t-1}$	-0.19 [-0.74, 0.36]	0.92 [0.01, 1.87]
$X_t \sim a_0 + a_1 X_{t-1} + \beta_1 Precip_{t-1}$	-	1.14 [0.24, 1.15]
$X_t \sim a_0 + a_1 X_{t-1} + a_2 X_{t-2}$	-0.46 [-1.02, 0.01]	-
$X_t \sim a_0 + a_1 X_{t-1}$	-	-
$X_t \sim a_0 + \beta_1 Precip_{t-1}$	-	1.37 [0.45, 2.28]
$X_t \sim a_0$	-	-

Table 5.2. Results of Bayesian state space time series model selection, by period of series analyzed and the process model structure. Change in WAIC relative to the best model (ΔWAIC), WAIC, and parameter estimates with 95% posterior intervals are shown. WAIC values within ΔWAIC <2 of the best model are bolded, and the best model is bolded. Parameter estimates the 95% posterior intervals which do not overlap zero are bolded as well.

Series	Original	Whole series, fitted β_1	Part I, fitted β_1	Part II, fitted β_1	Whole series, equal β_1	Part I, equal β_1	Part II, equal β_1	Part II, no a_1, a_2
Original	0							
Whole series, fitted β_1	22.14	0						
Part I, fitted β_1	22.80	10.38	0					
Part II, fitted β_1	**17.55**	10.17	16.51	0				
Whole series, equal β_1	18.54	11.87	15.89	11.30	0			
Part I, equal β_1	21.42	19.56	18.19	16.44	17.58	0		
Part II, equal β_1	**17.55**	10.17	16.51	0	6.22	16.5	0	
Part II, no a_1, a_2	19.72	12.73	15.84	6.52	6.37	13.75	6.67	0

Table 5.3. Dissimilarity matrix of simulated time series from fitted state-space process models, with original fitted parameters and with effect of precipitation set to equal at the highest fitted value (β_1=0.922), all compared with the original observed time series. Lowest dissimilarities relative to the original series for simulations with fitted or equal β_1 values are bolded.

6. Conclusion

In this dissertation, I have illustrated some of the diverse ways that climate can impact species interactions and population dynamics with the case study of the Ranchman's tiger moth (*Arctia virginalis*). I also developed theory that I hope has some utility to others studying the biotic impacts of climate change. In Chapter I, I developed a framework to analyze how thermal asymmetries may affect predator-prey interactions in stage- or size-dependent interactions. In this case, more rapid prey development did not compensate for increased attack rate of predators, resulting in lower prey survival with warming. In Chapter II, I expanded the work in Chapter I to examine how thermal asymmetries, predator diversity, and thermal niche traits affect the importance of direct vs. indirect effects of warming in ectotherm communities. From empirical and theoretical results, I predict that indirect effects of warming should have reduced significance in more diverse and complementary communities. In Chapter III, I showed that infection by a granulovirus causes significant mortality in *Arctia virginalis* caterpillars, and is delayed density-dependent, providing a mechanism for second-order dynamics in this species. I also showed for the first time in a field setting that ultraviolet radiation attenuates viral infection severity, which is something that is expected based on viral biology. In Chapter IV, I showed that second-order dynamics driven by viral infection interacts with precipitation dynamics. These transient interactions resulted in a shift from short-period cycles to long-period population cycles of *Arctia virginalis* as precipitation patterns in California shifted from wetter to periodic long drought. I argue that this is the first empirical demonstration of stochastic resonance, a process that has been hypothesized to exist since the work of Royama (1992).

Overall, I believe that my work has provided significant new insight in the population dynamics of *Arctia virginalis,* founded on the 35-plus year history of study of this species by my

co-advisor, Richard Karban. Through this work, I have developed what I hope will be useful predictive theory for understanding the impacts of climate change on natural communities. This is a direction that I am excited to continue to pursue: I see it as a research direction that both addresses pressing issues for our planet and is an excellent avenue to uncover basic insights about the natural world.

7. References

Akhanaev, Y. B., I. A. Belousova, N. I. Ershov, M. Nakai, V. V Martemyanov, and V. V Glupov. 2017. Comparison of tolerance to sunlight between spatially distant and genetically different strains of Lymantria dispar nucleopolyhedrovirus. Plos One 12:e0189992.

Alonso, D., A. J. McKane, and M. Pascual. 2007. Stochastic amplification in epidemics. Journal of the Royal Society Interface 4:575–582.

Amarasekare, P. 2015. Effects of temperature on consumer-resource interactions. Journal of Animal Ecology 84:665–679.

Amarasekare, P., and R. Sifuentes. 2012. Elucidating the temperature response of survivorship in insects. Functional Ecology 26:959–968.

Anderson, M. T., J. M. Kiesecker, D. P. Chivers, and A. R. Blaustein. 2001. The direct and indirect effects of temperature on a predator– prey relationship. Canadian Journal of Zoology 79:1834–1841.

Anderson, R. M., and R. M. May. 1980. Infectious Diseases and Population Cycles of Forest Insects. Science 210:658–661.

Anderson, R. M., and R. M. May. 1981. The population dynamics of microparasites and their invertebrate hosts. Philosophical Transactions of the Royal Society B: Biological Sciences 291:451–519.

Andrewartha, H. G., and L. C. Birch. 1954. The distribution and abundance of animals. University of Chicago Press.

Angilletta Jr, M. J., P. H. Niewiarowski, and C. A. Navas. 2002. The evolution of thermal physiology in ectotherms. Journal of Thermal Biology 27:249–268.

Antonio, F. D. N., and J. L. A. M. Stigler. 2009. tsDyn: Time series analysis based on dynamical

systems theory.

Arnaud, P. H. 1978. Host Parasite Catalog of North American Tachinidae (Diptera). Department of Agriculture, Science and Education Administration.

Bale, J. S., G. J. Masters, I. D. Hodkinson, C. Awmack, T. M. Bezemer, V. K. Brown, J. Butterfield, A. Buse, J. C. Coulson, J. Farrar, J. E. G. Good, R. Harrington, S. Hartley, T. H. Jones, R. L. Lindroth, M. C. Press, I. Symrnioudis, A. D. Watt, and J. B. Whittaker. 2002. Herbivory in global climate change research: Direct effects of rising temperature on insect herbivores. Global Change Biology 8:1–16.

Barraquand, F., S. Louca, K. C. Abbott, C. A. Cobbold, F. Cordoleani, D. L. DeAngelis, B. D. Elderd, J. W. Fox, P. Greenwood, F. M. Hilker, D. L. Murray, C. R. Stieha, R. A. Taylor, K. Vitense, G. S. K. Wolkowicz, and R. C. Tyson. 2017. Moving forward in circles: challenges and opportunities in modelling population cycles. Ecology Letters 20:1074–1092.

Barrett, J. W., A. J. Brownwright, M. J. Primavera, and S. R. Palli. 1998. Studies of the nucleopolyhedrovirus infection process in insects by using the green fluorescence protein as a reporter. Journal of Virology 72:3377–3382.

Barton, B. T., and O. J. Schmitz. 2009. Experimental warming transforms multiple predator effects in a grassland food web. Ecology Letters 12:1317–1325.

Bates, D., M. Maechler, B. Bolker, and S. Walker. 2014. lme4: Linear mixed-effects models using Eigen and S4.

Beisner, B. E., E. McCauley, and F. J. Wrona. 1997. The influence of temperature and food chain length on plankton predator-prey dynamics. Canadian Journal of Fisheries and Aquatic Sciences 54:586–595.

Benrey, B., and R. F. Denno. 1997. The slow-growth--high-mortality hypothesis : A test using

the cabbage butterfly. Ecology 78:987–999.

Berlow, E. L., J. A. Dunne, N. D. Martinez, P. B. Stark, R. J. Williams, and U. Brose. 2009. Simple prediction of interaction strengths in complex food webs. Proceedings of the National Academy of Sciences 106:187–91.

Berryman, A. A. 1996. What causes population cycles of forest Lepidoptera? Trends in Ecology and Evolution 11:28–32.

Berryman, A. A. 2002. Population cycles: the case for trophic interactions. Page (A. A. Berryman, Ed.). Oxford University Press, New York.

Bjørnstad, O. N., M. Begon, N. C. Stenseth, W. Falck, S. M. Sait, and D. J. Thompson. 1998. Population dynamics of the indian meal moth: Demographic stochasticity and delayed regulatory mechanisms. Journal of Animal Ecology 67:110–126.

Bjørnstad, O. N., and B. T. Grenfell. 2001. Noisy clockwork: time series analysis of population fluctuations in animals. Science 293:638–43.

Brooker, R. W. 2006. Plant-plant interactions and environmental change. New Phytologist 171:271–284.

Brooks, M. E., K. Kristensen, K. J. van Benthem, A. Magnusson, C. W. Berg, A. Nielsen, H. J. Skaug, M. Mächler, and B. M. Bolker. 2017. glmmTMB balances speed and flexibility among packages for zero-inflated generalized linear mixed modeling. R Journal 9:378–400.

Brose, U. 2010. Body-mass constraints on foraging behaviour determine population and food-web dynamics. Functional Ecology 24:28–34.

Brown, J. H., J. F. Gillooly, A. P. Allen, V. M. Savage, and G. B. West. 2004. Toward a metabolic theory of ecology. Ecology 85:1771–1789.

Burden, J. P., C. M. Griffiths, J. S. Cory, P. Smith, and S. M. Sait. 2002. Vertical transmission of

sublethal granulovirus infection in the Indian meal moth, Plodia interpunctella. Molecular Ecology 11:547–555.

Burthe, S., S. Telfer, X. Lambin, M. Bennett, D. Carslake, A. Smith, and M. Begon. 2006. Cowpox virus infection in natural field vole Microtus agrestis populations: Delayed density dependence and individual risk. Journal of Animal Ecology 75:1416–1425.

Cabodevilla, O., E. Villar, C. Virto, R. Murillo, T. Williams, and P. Caballero. 2011. Intra- and intergenerational persistence of an insect nucleopolyhedrovirus: Adverse effects of sublethal disease on host development, reproduction, and susceptibility to superinfection. Applied and Environmental Microbiology 77:2954–2960.

Cazelles, B., M. Chavez, A. J. McMichael, and S. Hales. 2005. Nonstationary influence of El Niño on the synchronous dengue epidemics in Thailand. PLoS Medicine 2:0313–0318.

Chapin, F. S., B. H. Walker, R. J. Hobbs, D. U. Hooper, J. H. Lawton, O. E. Sala, and D. Tilman. 1997. Biotic Control over the Functioning of Ecosystems. Science 277:500–504.

Christensen, B. 1996. Predator foraging capabilities and prey antipredator behaviours : pre- versus postcapture constraints on size-dependent predator-prey interactions. Oikos 76:368–380.

Christensen, R. H. B. 2019. ordinal—Regression Models for Ordinal Data.

Clark, J. S., S. R. Carpenter, M. Barber, S. Collins, A. Dobson, J. A. Foley, D. M. Lodge, M. Pascual, R. Pielke, and W. Pizer. 2001. Ecological forecasts: an emerging imperative. Science 293:657–660.

Cloern, J. E., K. A. Hieb, T. Jacobson, B. Sans, E. Di Lorenzo, M. T. Stacey, J. L. Largier, W. Meiring, W. T. Peterson, T. M. Powell, M. Winder, and A. D. Jassby. 2010. Biological communities in San Francisco Bay track large-scale climate forcing over the North Pacific.

Geophysical Research Letters 37:1–6.

Cornulier, T., N. G. Yoccoz, V. Bretagnolle, J. E. Brommer, A. Butet, F. Ecke, D. A. Elston, E. Framstad, H. Henttonen, B. Hörnfeldt, O. Huitu, C. Imholt, R. A. Ims, J. Jacob, B. Jędrzejewska, A. Millon, S. J. Petty, H. Pietiäinen, E. Tkadlec, K. Zub, and X. Lambin. 2013. Europe-wide dampening of population cycles in keystone herbivores. Science 340:63–66.

Cory, J. S. 2015. Insect virus transmission: different routes to persistence. Current Opinion in Insect Science 8:130–135.

Cory, J. S., and J. H. Myers. 2003. The Ecology and Evolution of Insect Baculoviruses. Annual Review of Ecology, Evolution, and Systematics 34:239–272.

Coumou, D., and S. Rahmstorf. 2012. A decade of weather extremes. Nature Climate Change 2:491–496.

Cramer, W., A. Bondeau, F. I. Woodward, I. C. Prentice, R. A. Betts, V. Brovkin, P. M. Cox, V. Fisher, J. A. Foley, A. D. Friend, C. Kucharik, M. R. Lomas, N. Ramankutty, S. Sitch, B. Smith, A. White, and C. Young-Molling. 2001. Global response of terrestrial ecosystem structure and function to CO2 and climate change: Results from six dynamic global vegetation models. Global Change Biology 7:357–373.

Culler, L. E., M. P. Ayres, R. A. Virginia, and L. E. Culler. 2015. In a warmer Arctic , mosquitoes avoid increased mortality from predators by growing faster. Proceedings of the Royal Society B: Biological Sciences 282:20151549.

Dell, A. I., S. Pawar, and V. M. Savage. 2011. Systematic variation in the temperature dependence of physiological and ecological traits. Proceedings of the National Academy of Sciences 108:10591–10596.

Dell, A. I., S. Pawar, and V. M. Savage. 2014. Temperature dependence of trophic interactions are driven by asymmetry of species responses and foraging strategy. Journal of Animal Ecology 83:70–84.

Deutsch, C. A., J. J. Tewksbury, R. B. Huey, K. S. Sheldon, C. K. Ghalambor, D. C. Haak, and P. R. Martin. 2008. Impacts of climate warming on terrestrial ectotherms across latitude. Proceedings of the National Academy of Sciences 105:6668–6672.

Deutsch, C. A., J. J. Tewksbury, M. Tigchelaar, D. S. Battisti, S. C. Merrill, R. B. Huey, and R. L. Naylor. 2018. Increase in crop losses to insect pests in a warming climate. Science 361:916–919.

Dietze, M. C. 2017. Prediction in ecology: a first-principles framework. Ecological Applications 27:2048–2060.

Duan, J. J., D. E. Jennings, D. C. Williams, and K. M. Larson. 2014. Patterns of parasitoid host utilization and development across a range of temperatures: implications for biological control of an invasive forest pest. BioControl 59:659–669.

Eberle, K. E., S. Asser-Kaiser, S. M. Sayed, H. T. Nguyen, and J. A. Jehle. 2008. Overcoming the resistance of codling moth against conventional Cydia pomonella granulovirus (CpGV-M) by a new isolate CpGV-I12. Journal of Invertebrate Pathology 98:293–298.

Elderd, B. D., and J. R. Reilly. 2014. Warmer temperatures increase disease transmission and outbreak intensity in a host-pathogen system. Journal of Animal Ecology 83:838–849.

Elliott, J. M. 1982. The effects of temperature and ration size on the growth and energetics of salmonids in captivity. Comparative Biochemistry and Physiology Part B: Comparative Biochemistry 73:81–91.

Elton, C., and M. Nicholson. 1942. The ten-year cycle in numbers of the lynx in Canada. Journal

of Animal Ecology:215–244.

English-Loeb, G. M., A. K. Brody, and R. Karban. 1993. Host-Plant-Mediated Interactions between a Generalist Folivore and its Tachinid Parasitoid. Journal of Animal Ecology 62:465.

English-Loeb, G. M., R. Karban, and A. K. Brody. 1990. Arctiid larvae survive attack by a tachinid parasitoid and produce viable offspring. Ecological Entomology 15:361–362.

Englund, G., G. Öhlund, C. L. Hein, and S. Diehl. 2011. Temperature dependence of the functional response. Ecology Letters 14:914–921.

Fleming, S. B., J. Kalmakoff, R. D. Archibald, and K. M. Stewart. 1986. Density-dependent virus mortality in populations of Wiseana (Lepidoptera: Hepialidae). Journal of Invertebrate Pathology 48:193–198.

Fussmann, K. E., F. Schwarzmüller, U. Brose, A. Jousset, and B. C. Rall. 2014. Ecological stability in response to warming. Nature Climate Change 4:206–210.

Fuxa, J. R. 2004. Ecology of insect nucleopolyhedroviruses. Agriculture, Ecosystems & Environment 103:27–43.

Garnier, S. 2018. viridis: Default Color Maps from “matplotlib.”

Gelman, A., and D. B. Rubin. 1992. Inference from iterative simulation using multiple sequences. Statistical Science 7:457–472.

Gillooly, J. F., J. H. Brown, G. B. West, V. M. Savage, and E. L. Charnov. 2001. Effects of size and temperature on metabolic rate. Science 293:2248–51.

Gouhier, T. C., A. Grinsted, and V. Simko. 2019. R package biwavelet: Conduct Univariate and Bivariate Wavelet Analyses.

Grace, J. B., D. J. Johnson, J. S. Lefcheck, and J. E. K. Byrnes. 2018. Quantifying relative

importance: computing standardized effects in models with binary outcomes. Ecosphere 9:e02283.

Greenman, J. V., and T. G. Benton. 2003. The amplification of environmental noise in population models: Causes and consequences. American Naturalist 161:225–239.

Greenslade, P. J. M. 1973. Sampling ants with pitfall traps: digging-in effects. Insectes Sociaux 20:343–353.

Griego, V. M., M. E. Martignoni, and A. E. Claycomb. 1985. Inactivation of nuclear polyhedrosis virus (Baculovirus subgroup A) by monochromatic UV radiation. Applied and Environmental Microbiology 49:709–710.

Grof-Tisza, P., M. Holyoak, E. H. Antell, and R. Karban. 2014. Predation and associational refuge drive ontogenetic niche shifts in an arctiid caterpillar. Ecology 96:140703220532006.

Harrison, X. A. 2014. Using observation-level random effects to model overdispersion in count data in ecology and evolution. PeerJ 2:e616.

Haynes, K. J., J. C. Tardif, and D. Parry. 2018. Drought and surface-level solar radiation predict the severity of outbreaks of a widespread defoliating insect. Ecosphere 9.

Hoekman, D. 2010. Turning up the heat : Temperature influences the relative importance of top-down and bottom-up effects. Ecology 91:2819–2825.

Hovila, J., A. Arola, and J. Tamminen. 2014. OMI/Aura Surface UVB Irradiance and Erythemal Dose Daily L2 Global Gridded 0.25 degree x 0.25 degree V3,. NASA Goddard Space Flight Center, Goddard Earth Sciences Data and Information Services Center.

Ims, R. A., J. A. Henden, and S. T. Killengreen. 2008. Collapsing population cycles. Trends in Ecology and Evolution 23:79–86.

Janzen, D. H. 1967. Why mountain passes are higher in the tropics. The American Naturalist 101:233–249.

Jeffs, C. T., and O. T. Lewis. 2013. Effects of climate warming on host-parasitoid interactions. Ecological Entomology 38:209–218.

Karban, R., P. Grof-Tisza, and M. Holyoak. 2017. Wet years have more caterpillars: Interacting roles of plant litter and predation by ants. Ecology.

Karban, R., P. Grof-Tisza, M. McMunn, H. Kharouba, and M. Huntzinger. 2015. Caterpillars escape predation in habitat and thermal refuges. Ecological Entomology 40:725–731.

Karban, R., C. Karban, M. Huntzinger, I. Pearse, and G. Crutsinger. 2010. Diet mixing enhances the performance of a generalist caterpillar, Platyprepia virginalis. Ecological Entomology 35:92–99.

Karban, R., T. M. Mata, P. Grof-Tisza, G. Crutsinger, and M. A. Holyoak. 2013. Non-trophic effects of litter reduce ant predation and determine caterpillar survival and distribution. Oikos 122:1362–1370.

Karban, R., and P. de Valpine. 2010. Population dynamics of an Arctiid caterpillar-tachinid parasitoid system using state-space models. Journal of Animal Ecology 79:650–661.

Kaspari, M., N. A. Clay, J. Lucas, S. P. Yanoviak, and A. Kay. 2015. Thermal adaptation generates a diversity of thermal limits in a rainforest ant community. Global Change Biology 21:1092–1102.

Killengreen, S. T., and R. A. Ims. 2008. Collapsing population cycles:79–86.

Kingsolver, J. G. 2009. The well-temperatured biologist. The American Naturalist 174:755–768.

Kingsolver, J. G., H. Arthur Woods, L. B. Buckley, K. A. Potter, H. J. MacLean, and J. K. Higgins. 2011. Complex life cycles and the responses of insects to climate change.

Integrative and Comparative Biology 51:719–732.

Kingsolver, J. G., and R. B. Huey. 2008. Size, temperature, and fitness : three rules. Evolutionary Ecology Research 10:251–268.

Kruschke, J. 2014. Doing Bayesian data analysis: A tutorial with R, JAGS, and Stan.

Kühsel, S., and N. Blüthgen. 2015. High diversity stabilizes the thermal resilience of pollinator communities in intensively managed grasslands. Nature Communications 6:2–9.

Lacey, L. A., and L. F. Solter. 2012. Initial handling and diagnosis of diseased invertebrates. Pages 1–14 *in* L. A. Lacey, editor. Manual of techniques in invertebrate pathology. 2nd edition. Elsevier Ltd., London, United Kingdom.

Lang, B., B. C. Rall, and U. Brose. 2012. Warming effects on consumption and intraspecific interference competition depend on predator metabolism. Journal of Animal Ecology 81:516–523.

Lawton, J. H. 1992. There are not 10 million kinds of population dynamics. Oikos 63:337–338.

Lefcheck, J. S. 2016. piecewiseSEM: Piecewise structural equation modelling in r for ecology, evolution, and systematics. Methods in Ecology and Evolution 7:573–579.

Li, H., M. Kanamitsu, S. Y. Hong, K. Yoshimura, D. R. Cayan, V. Misra, and L. Sun. 2014. Projected climate change scenario over California by a regional ocean–atmosphere coupled model system. Climatic Change 122:609–619.

Louthan, A. M., D. F. Doak, and A. L. Angert. 2015. Where and when do species interactions set range limits? Trends in Ecology and Evolution 30:780–792.

Lüdecke, D. 2018. ggeffects: Tidy data frames of marginal effects from regression models. Journal of Open Source Software 3:772.

Martyn, A., N. Best, K. Cowles, K. Vines, D. Bates, R. Almond, and A. Magnusson. 2019.

Package ‘ coda ’: Output Analysis and Diagnostics for MCMC.

Matthews, H. J., I. Smith, and J. P. Edwards. 2002. Lethal and sublethal effects of a granulovirus on the tomato moth Lacanobia oleracea. Journal of Invertebrate Pathology 80:73–80.

May, R. M. 1973. Time-delay versus stability in population models with two and three trophic levels. Ecology 54:315–325.

McMunn, M. S. 2017. A time-sorting pitfall trap and temperature datalogger for the sampling of surface-active arthropods. HardwareX 1:38–45.

Mittelbach, G. G. . 1981. Foraging efficiency and body size : A study of optimal diet and habitat use by bluegills. Ecology 62:1370–1386.

Mittelbach, G. G., D. W. Schemske, H. V Cornell, A. P. Allen, J. M. Brown, M. B. Bush, S. P. Harrison, A. H. Hurlbert, N. Knowlton, and H. A. Lessios. 2007. Evolution and the latitudinal diversity gradient: speciation, extinction and biogeography. Ecology Letters 10:315–331.

Myers, J. H. 2000. Population fluctuations of the western tent caterpillar in southwestern British Columbia. Population Ecology 42:231–241.

Myers, J. H., and J. S. Cory. 2013. Population Cycles in Forest Lepidoptera Revisited. Annual Review of Ecology, Evolution, and Systematics 44:565–592.

Myers, J. H., and J. S. Cory. 2016. Ecology and evolution of pathogens in natural populations of Lepidoptera. Evolutionary Applications 9:231–247.

Nicholson, A. J. 1933. The balance of animal populations. Journal of Animal Ecology 2:132 – 178.

NREL. 2009. NREL GIS Data: Continental United States Global Horizontal Solar Resource 10km Resolution (1998 - 2005). ttps://catalog.data.gov/dataset/nrel-gis-data-continental-

united-states-global-horizontal-solar-resource-10km-resolution-1.

O'Connor, M. I., M. F. Piehler, D. M. Leech, A. Anton, and J. F. Bruno. 2009. Warming and resource availability shift food web structure and metabolism. PLoS Biology 7:3–8.

Ohlund, G., P. Hedstrom, S. Norman, C. L. Hein, and G. Englund. 2014. Temperature dependence of predation depends on the relative performance of predators and prey. Proceedings of the Royal Society B: Biological Sciences 282:20142254–20142254.

Olofsson, E. 1988. Environmental persistence of the nuclear polyhedrosis virus of the European pine sawfly in relation to epizootics in Swedish Scots pine forests. Journal of Invertebrate Pathology 52:119–129.

Paine, T. 1976. Size-limited predation : An observational and experimental approach with the Mytilus- isaster interaction. Ecology 57:858–873.

Parmesan, C. 2006. Ecological and evolutionary responses to recent climate change. Annual Review of Ecology Evolution and Systematics 37:637–669.

Pepi, A., P. Grof-Tisza, M. Holyoak, and R. Karban. 2018. As temperature increases, predator attack rate is more important to survival than a smaller window of prey vulnerability. Ecology 99:1584–1590.

Pepi, A., M. Holyoak, and R. Karban. 2021a. Altered precipitation dynamics lead to a shift in herbivore dynamical regime. Ecology Letters.

Pepi, A., and M. McMunn. 2021. Predator Diversity and Thermal Niche Complementarity Attenuate Indirect Effects of Warming on Prey Survival. The American Naturalist 198:000–000.

Pepi, A., V. Pan, and R. Karban. 2021b. Influence of delayed density and ultraviolet radiation on caterpillar granulovirus infection and mortality. bioRxiv:2021.03.22.436482.

Petchey, O. L., U. Brose, and B. C. Rall. 2010. Predicting the effects of temperature on food web connectance. Philosophical Transactions of the Royal Society B: Biological Sciences 365:2081–2091.

Petchey, O. L., P. T. McPhearson, T. M. Casey, and P. J. Morin. 1999. Environmental warming alters food-web structure and ecosystem function. Nature 402:69–72.

Pinheiro, J., D. Bates, S. DebRoy, D. Sarkar, and R. D. C. Team. 2019. nlme: Linear and nonlinear mixed effects models.

Plummer, M. 2019. rjags: Bayesian Graphical Models using MCMC.

Post, E. 2013. Ecology of climate change: the importance of biotic interactions. Princeton University Press, Princeton.

Post, E., and M. C. Forchhammer. 2002. Synchronization of animal population dynamics by large-scale climate. Nature 420:168–171.

Prather, R. M., K. A. Roeder, N. J. Sanders, and M. Kaspari. 2018. Using metabolic and thermal ecology to predict temperature dependent ecosystem activity: a test with prairie ants. Ecology 99:2113–2121.

R Development Core Team. 2020. R: A Language and Environment for Statistical Computing. R Foundation for Statistical Computing, Vienna, Austria.

Rall, B. C., O. Vucic-Pestic, R. B. Ehnes, M. Emmerson, and U. Brose. 2010. Temperature, predator-prey interaction strength and population stability. Global Change Biology 16:2145–2157.

Ranta, E., P. Lundberg, V. Kaitala, and J. Laakso. 2000. Visibility of the environmental noise modulating population dynamics. Proceedings of the Royal Society B: Biological Sciences 267:1851–1856.

Rodó, X., M. Pascual, G. Fuchs, and A. S. G. Faruque. 2002. ENSO and cholera: A nonstationary link related to climate change? Proceedings of the National Academy of Sciences of the United States of America 99:12901–12906.

Roland, J., and W. J. Kaupp. 1995. Reduced transmission of forest tent caterpillar (Lepidoptera: Lasiocampidae) nuclear polyhedrosis virus at the forest edge. Environmental Entomology 24:1175–1178.

Rothman, L. D. 1997. Immediate and delayed effects of a viral pathogen and density on tent caterpillar performance. Ecology 78:1481–1493.

Rouyer, T., J.-M. Fromentin, N. C. Stenseth, and B. Cazelles. 2008. Analysing multiple time series and extending significance testing in wavelet analysis. Marine Ecology Progress Series 359:11–23.

Royama, T. 1992. Analytical Population Dynamics. Chapman & Hall, London.

Sagripanti, J. L., and C. D. Lytle. 2007. Inactivation of influenza virus by solar radiation. Photochemistry and Photobiology 83:1278–1282.

Scaven, V. L., and N. E. Rafferty. 2013. Physiological effects of climate warming on flowering plants and insect pollinators and potential consequences for their interactions. Current Zoology 59:419–426.

Shipley, B. 2000. A New Inferential Test for Path Models Based on Directed Acyclic Graphs A New Inferential Test for Path Models Based on Directed Acyclic Graphs. Structural Equation Modelling 7:206–218.

Simon Wang, S. Y., J. H. Yoon, E. Becker, and R. Gillies. 2017. California from drought to deluge. Nature Climate Change 7:465–468.

Stigler, M. 2019. seglm: Segmented/threshold regression methods.

Swain, D. L., B. Langenbrunner, J. D. Neelin, and A. Hall. 2018. Increasing precipitation volatility in twenty-first-century California. Nature Climate Change 8:427–433.

Sweeney, B. W., D. H. Funk, A. A. Camp, D. B. Buchwalter, and J. K. Jackson. 2018. Why adult mayflies of *Cloeon dipterum* (Ephemeroptera:Baetidae) become smaller as temperature warms. Freshwater Science 37:64–81.

Taylor, D. L., and J. S. Collie. 2003. A temperature- and size-dependent model of sand shrimp (Crangon septemspinosa) predation on juvenile winter flounder (Pseudopleuronectes americanus). Canadian Journal of Fisheries and Aquatic Sciences 60:1133–1148.

Taylor, F. 1981. Ecology and evolution of physiological time in insects. American Naturalist 117:1–23.

Thomson, J. R., W. J. Kimmerer, L. R. Brown, K. B. Newman, R. Mac Nally, W. A. Bennett, F. Feyrer, and E. Fleishman. 2010. Bayesian change point analysis of abundance trends for pelagic fishes in the upper San Francisco Estuary. Ecological Applications 20:1431–1448.

Tilman, D. 1982. Resource competition and community structure. Princeton University Press., Princeton, New Jersey.

Tomé, T., and M. J. De Oliveira. 2009. Role of noise in population dynamics cycles. Physical Review E - Statistical, Nonlinear, and Soft Matter Physics 79:1–8.

Turchin, P. 1990. Rarity of density dependence or population regulation with lags? Nature 344:660–663.

Turchin, P. 2003. Complex Population Dynamics: A Theoretical/Empirical Synthesis. Princeton University Press, Princeton.

Tylianakis, J. M., R. K. Didham, J. Bascompte, and D. A. Wardle. 2008. Global change and species interactions in terrestrial ecosystems. Ecology Letters 11:1351–1363.

Uszko, W., S. Diehl, G. Englund, and P. Amarasekare. 2017. Effects of warming on predator-prey interactions - a resource-based approach and a theoretical synthesis. Ecology Letters 20:513–523.

Vasseur, D. A., and K. S. McCann. 2005. A mechanistic approach for modeling temperature-dependent consumer-resource dynamics. American Naturalist 166:184–198.

Vega, F. E., and H. K. Kaya. 2012. Insect pathology. Academic press.

Vehtari, A., A. Gelman, and J. Gabry. 2017. Practical Bayesian model evaluation using leave-one-out cross-validation and WAIC. Statistics and Computing 27:1413–1432.

Vucic-Pestic, O., R. B. Ehnes, B. C. Rall, and U. Brose. 2011. Warming up the system: Higher predator feeding rates but lower energetic efficiencies. Global Change Biology 17:1301–1310.

Walther, G., E. Post, P. Convey, A. Menzel, C. Parmesan, T. J. C. Beebee, J. Fromentin, O. H. I, and F. Bairlein. 2002. Ecological responses to recent climate change. Nature 416:389–395.

Ward, S. F., B. H. Aukema, S. Fei, and A. M. Liebhold. 2020. Warm temperatures increase population growth of a nonnative defoliator and inhibit demographic responses by parasitoids. Ecology:e03156.

Weare, B. C. 2009. How will changes in global climate influence California? California Agriculture 63:59–66.

Werner, E. E. 1986. Amphibian metamorphosis: Growth rate, predation risk, and the optimal size at transformation. American Naturalist 128:765–770.

Wickham, H. 2009. ggplot2: elegant graphics for data analysis. Springer, New York.

Wickham, H. 2016. ggplot2: Elegant Graphics for Data Analysis. Springer-Verlag New York.

Wild, M. 2016. Decadal changes in radiative fluxes at land and ocean surfaces and their

relevance for global warming. Wiley Interdisciplinary Reviews: Climate Change 7:91–107.

Witt, D. J., and G. R. Stairs. 1975. The effects of ultraviolet irradiation on a Baculovirus infecting Galleria mellonella. Journal of Invertebrate Pathology 26:321–327.

Yu-Sung Su, and M. Yajima. 2015. R2jags: Using R to Run "JAGS."

Zvereva, E. L., and M. V. Kozlov. 2006. Consequences of simultaneous elevation of carbon dioxide and temperature for plant-herbivore interactions: A metaanalysis. Global Change Biology 12:27–41.